Journal of Cleaner Production 436 (2024) 140577

Contents lists available at ScienceDirect

Journal of Cleaner Production

journal homepage: www.elsevier.com/locate/jclepro

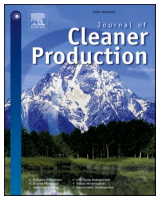

Impact of hybrid nano PCM (paraffin wax with Al_2O_3 and ZnO nanoparticles) on photovoltaic thermal system: Energy, exergy, exergoeconomic and enviroeconomic analysis

Md. Golam Kibria [a,*], Md. Shahriar Mohtasim [a], Utpol K. Paul [a], Barun K. Das [b], R. Saidur [c]

[a] Department of Mechanical Engineering, Rajshahi University of Engineering and Technology (RUET), Rajshahi 6204, Bangladesh
[b] School of Engineering, Edith Cowan University, Joondalup, WA-6027, Australia
[c] Research Centre for Nano-Materials and Energy Technology, School of Engineering and Technology, Sunway University, Bandar Sunway, Malaysia

ARTICLE INFO

Handling Editor: Jin-Kuk Kim

Keywords:
Photovoltaic thermal (PVT)
Hybrid nano-PCM
Exergy analysis
Environmental analysis
Economic analysis

ABSTRACT

Global renewable energy efforts place a significant preference on substantial solar photovoltaic (PV) systems. Photovoltaic thermal (PVT) systems are the upgraded version of PV modules that concurrently produce both electricity and heat. Hybrid nano-particles (2.0 wt % ZnO and 2.0 wt % Al_2O_3) into the phase change material (PCM) known as HNPCM system has been introduced in this current study for enhancing the electrical and thermal performance of the PVT system by improving the thermophysical properties of paraffin wax as used for passive cooling. Three PV systems were compared in terms of performance: a conventional PV system, a PVT system using paraffin wax as a PCM (PVT/PCM), and a PVT system with 2.0 wt % of Al_2O_3 and ZnO in PCM (PVT/HNPCM). Upon investigation, the PVT/HNPCM system under outdoor environmental condition shows that the inclusion of different nanoparticles in PCM led to improvements in thermal and overall efficiency of 17.32 % and 13.82 % compared to PVT/PCM, respectively. This results in increase of electrical efficiency of 34.84 % when compared to conventional PV panel and incremental peak exergy efficiency of 36.47 %. Besides, for PVT/HNPCM, cost of electricity production ($/kWh) is almost 16.67 % less than the conventional PV configuration and the payback time is about 2.1 years on the overall exergy basis. Additionally, PVT/HNPCM system exhibits the long-term life cycle conversion efficiency compared to conventional PV panel and maximum sustainability index of 1.21 has been also found. Finally, the conclusion can be drawn positively for PVT/HNPCM as the most effective system from the exergy efficiency, exergy cost, and CO_2 avoidance rates point of view.

1. Introduction

Recently, the demand for energy is increasing rapidly around the globe resulting in the dependency on fossil fuels, especially for electrical energy which causes the depletion of these resources. On the other hand, mitigation of global warming and reducing CO_2 emissions to the environment have been the burning issues to move towards alternative sources of energy rather than fossil fuels (Jiakui et al., 2023). The necessity to take use of renewable energy sources and environmentally conscious practices has greatly increased in light of the problems associated with environmental deterioration and a dramatic drop in the quality and quantity of natural resources (Nasr Esfahani et al., 2023). However, the sun transmits an electromagnetic radiation that carries sufficient amount of energy and the intensity of radiation (Shahverdian et al., 2023). This energy can be harnessed and converted into a useful form of energy i.e. electricity by using photovoltaic (PV) panels. Though the photovoltaic panel has the ability to convert solar energy into electricity, it exhibits drawbacks of its lower efficiency, and efficiency decreases with an elevation of PV surface temperature. A study showed that output power is declined by approximately 0.65–0.80 % by elevating per degree Celsius of temperature of PV cell (Abdulmunem et al., 2021). Therefore, it needs to adopt an effective cooling method to minimize the cell temperature and optimizes its electrical performance. There are two effective methods of cooling the PV cell viz. active and passive cooling. A fan, blower, or pump is used to pass the coolant (water or air) underneath the PV panel to extract the heat from PV cells in the case of active cooling. It is a simple and natural air or water-circulating method (Abdalla and Shahsavar, 2023), but it does not

* Corresponding author.
E-mail address: kibria@me.ruet.ac.bd (Md.G. Kibria).

https://doi.org/10.1016/j.jclepro.2024.140577
Received 2 September 2023; Received in revised form 19 December 2023; Accepted 2 January 2024
Available online 3 January 2024

significantly enhance the conversion efficiency as the circulating device consumes some of the output power. Hence, many researchers have focused on the passive cooling method using phase change material (PCM), extended surfaces (fin), heat pipe, and nano-fluid (Koohestani et al., 2023; Said et al., 2023a).

Among them, phase change material (Paraffin wax) is widely used due to its non-corrosive, non-toxic, and chemically stable attributes and its ability to store heat. There are numerous fields to utilize the PCM, such as it can be used in solar cell tracking systems (Allouhi et al., 2022), used in air absorption systems (Soliman et al., 2021). PCM is also applied in the HVAC system for building cooling and heating purposes. It acts as a thermal storage system in the HVAC system (Borri et al., 2021). Addition of CuO nano-particles inside the PCM can decline the time for solidifying of the PCM for storing energy at the charging time which improves the performance of the energy storage system (Said et al., 2023b; Sheikholeslami and Mahian, 2019). A study showed better performance for room space heating by using PCM embedded with aluminum foam which is situated at the backside of the radiator (Sardari et al., 2020). Now, phase change material is widely incorporated at the back side of the PV panel and it absorbs heat as a heat sink when the solar intensity is high. Thus, it declines the temperature of the surface of PV panel and improves the electrical efficiency. An experiment was done by Ejaz et al. (2022) using PT58 and RT44 as PCM with aluminum foam having 8 mm and 12 mm thickness and proved that the system having 12 mm thickness foam with RT44 PCM declined maximum cell temperature by about 24.39 °C and obtained highest conversion efficiency by about 12.06 %. Another study designed the multiple layer of PCM with varying melting point temperature in such a way that their melting point declines in the heat flow direction and this system prolonged the melting time of the PCM as well as thermal management duration of PV panel which optimize the power output (Mahdi et al., 2021). However, it has a drawback for its low thermal conductivity. Many researchers have focused on enhancing thermal conductivity of the PCM and eliminating the overheating problem of the PV panels. Thermal conductivity of the PCM can be enhanced by introducing nano-enhanced PCM (Nematpour Keshteli and Sheikholeslami, 2019) and overall performance of the PV panel can be enhanced by incorporating nano-fluid. Bassam et al. (2023) experimented using both nano-enhanced PCM (1 % SiC nano-particles) and nano-fluid (water/SiC) into the system which improved the thermal conductivity of the PCM as well as electrical and thermal performance. Another experimental investigation was carried out by Salem et al. (2019) using compound technique (Al_2O_3 nano-particles/PCM + water) through aluminum channel and obtained better performance of PV panel for electrical and thermal efficiency at 1 % of nano-particles. Jamil et al. (2023) used Silica (SiO_2) and Carbon Black (CB) nano-particles into PT-58 PCM for enhancing thermal conductivity and reduced cell temperatures by approximately 8.92 °C and 9.74 °C, respectively. Aluminum sheet acts as thermal conductivity enhancer (TCE) of PCM and the noticeable enhancement of electrical efficiency by about 2 % and reduction in cell temperature by about 10.35 °C were observed by incorporating PCM with aluminum sheet at back side of PV panels (M. et al., 2019). Yousef et al. (2022) used aluminum foam with paraffin and enhanced the energy and exergy efficiency than PV/PCM system. The outcomes exhibited the average energy and exergy efficiency in February by about 14 % and 14.97 % for PV-PCM/AF system than 13.84 % and 14.81 % respectively for PV/PCM system. PVT/nano-PCM exhibits better performance and the reduction in cell temperature occurs more than 4 °C than PVT-PCM system. The enhancement of overall energy and exergy efficiency was observed by around 3.30 % and 18.20 % respectively than PVT-PCM system, carried out by Islam et al. (2021). Another technology for cooling the PV cell temperature, proposed by Abdelrazik et al. (2022), is to use optical filtration (OF). This technology can diminish by about 42.10 % and 6.30 % of PV cell temperature respectively than conventional PV panels and PVT system. The usage of TiO_2-water nanofluid through the rectangular channel underneath the PV panel puts the positive impact on the performance of the system from exergetic point of view and exhibited the exergy efficiency about 12.68 % than 11.80 % for conventional PV panel which was carried out by Ould-Lahoucine et al. (2021). At first, the usage of PCM as passive cooling process and heating the place as per as requirement has been reported and analyzed. One of the major advantages of using PCM for cooling purpose for its excellent heat extraction ability and there is no requirement of external power sources. The extracted heat is utilized for the domestic purposes. The extracted heat is stored into the PCM and discharged it for the heating purposes of the place. The following section has reported and analyzed the usage of hybrid cooling technology for PV panels including nano-PCM with fin, nano-PCM with PVT systems etc. The advantages of hybrid cooling technology on the performance of the PV panels based on electrical, exergy, and thermal perspectives have also been highlighted. A comparison study was carried out between a reference PV, PVT with water, and PVT with TEG/nanofluid by Praveenkumar et al. (2023) and found that PV panel, PVT, and PVT/TEG/nanofluid having electrical efficiency of 11.64 %, 12.30 %, and 12.62 %, respectively. However, they had not yet conducted an energetic study, and they do not discuss how the suggested systems might behave sustainably. Gad et al. (2023) proposed a hybrid cooling system made up of flat heat pipes (HP) and PCM is explored to see how well PV can regulate their internal temperature. From that, the highest electrical, thermal and exergy efficiency were found about 11.50 %, 56.45 % and 14.98 %, respectively. However, the electrical efficiency was not much satisfactory compared to the previously published studies. Liu et al. (2023) conducted an experiment in China with a serpentine cooling tube with two different shapes to build a lab-scale PVT module and found that the electrical, thermal and exergy efficiency were 12.42 %, 45 % and 10.69 %, respectively. Table 1 shows the summary of recent published paper for improving the performance of PV panel based on energetic and exergetic point of view.

In this study, hybrid nano-particles have been integrated with the PCM in order to compensate for the low thermal conductivity and enhanced the rate of heat extraction from the PV surfaces. Some studies have focused on extended fins surfaces, water, or nano-fluid-based cooling methods, using PCM or single nano-particle with PCM for passive cooling of the PV panels. It is experimentally proved from some literature that using single nano-particle into PCM can enhance the thermal conductivity. Bayat et al. (2018) performed an experiment by using Al_2O_3 and copper oxide (CuO) nano-particles into paraffin wax with different weight percentage and exhibited that using 2.0 wt % of alumina improved thermal conductivity by around 12.50 % at testing condition 43 °C temperature. When CuO nanoparticles were hybridized with multi-walled carbon nanotube (MWCNT) and applied with paraffin wax, Kalbande et al. (2022) discovered that the increase in thermal conductivity was only 6.15 %. Incorporating Al_2O_3 nanoparticles with paraffin wax in a variety of wt % compositions, Chaichan and Kazem (2018) discovered that the increase in thermal conductivity for 2.0 wt % of Al_2O_3 with PCM was only 14.08 %. By integrating hybrid nanoparticles into PCM offers better thermophysical properties including enhanced thermal conductivity; therefore, the use of hybrid nanoparticles with PCM has a significant impact on temperature distribution throughout the PCM layers (Gad et al., 2023). The other benefits of using hybrid nanoparticles, including lower viscosity and cheaper cost. Laghari et al. (2022) employed sodium dodecylbenzene sulphonate (SDBS) as a surfactant and combined paraffin wax (PW) with a binary composite of titanium dioxide-graphene (TiO_2: Gr) (1 wt % TiO_2: 0.1, 0.5, 1 and 2.0 wt % of Graphene (Gr)) to increase the thermal conductivity of PCMs. The PW/TiO_2-1.0 and PW/TiO_2Gr-1.0 composite PCMs have thermal conductivities that are 120 % and 179 % more extensive, respectively, than base PW. Graphene nanoplatelet (GNP), and CuO were hybridized with Polyethylene Glycol 1500 (PCM) by Moein-Jahromi et al. (2022). The results displayed that the chemical mixture of GNP-CuO 3 % Nano-enhanced PCM (NePCM) had the lowest dynamic viscosity increase of 14.83 % and the maximum thermal conductivity enhancement of 91.81 % when contrasted with pure PCM. The hybrid

Table 1
Recent studies for the improvement of PV systems using different technologies.

System Configuration	System efficiency			Country	Year	Ref.
	Electrical energy	Thermal energy	Exergy			
A comparison study was carried out between a reference PV, PVT with water, and PVT with TEG/nanofluid.	PV panel, PVT, and PVT/TEG/nanofluid having electrical efficiency of 11.64 %, 12.30 %, and 12.62 %, respectively.	–	–	Russia	2023	Praveenkumar et al. (2023)
A hybrid cooling system made up of flat heat pipes (HP) and phase change material (PCM) is explored to see how well photovoltaic solar cells (PV) can regulate their internal temperature.	11.50 % and 9 % using SP31 and SP15-gel	56.45 %	14.98 %	–	2023	Gad et al. (2023)
A serpentine cooling tube with two different shapes had been employed to build a lab-scale photovoltaic/thermal module.	12.42 %	45–55 %	10.69 %	China	2023	Liu et al. (2023)
The finite volume approach was used to create a three-dimensional numerical model of the baffled-based PVT system, with pure water and SWCNT/Water nanofluid serving as the working fluids.	Almost 9.3 %	Almost 58 %	–	–	2022	Ahmadinejad et al. (2022)
Usage of paraffin/aluminum foam (AF) composite underneath the PV panel and comparative analysis with conventional PV and PV/PCM system.	Average efficiency in February, 14 %, 13.84 % and 13.40 % and in July, 13.09 %, 12.64 %, and 11.62 % for PV-PCM/AF, PV-PCM and PV panel	–	Average efficiency in February, 14.97 %, 14.81 % and 14.37 % and in July, 14.08 %, 13.57 %, and 12.50 % for PV-PCM/AF, PV-PCM and PV panel respectively.	Egypt	2022	Yousef et al. (2022)
Installation of two different collectors with PV panel viz. the serpentine (PV/T1) and the channeled (PV/T2) block.	9.74 % and 10.19 % for PV/T1 and PV/T2 respectively.	29.08 % and 49.68 % for PV/T1 and PV/T2 respectively.	10.64 %, and 11.53 % for PV/T1 and PV/T2 respectively.	Turkey	2021	Selimli et al. (2021)
Usage of fin and without fin in vertical PVT dryer with regulating air flowrate at 0.01, 0.012, and 0.014 kg/s respectively.	–	Maximum 71.96 % with fin at 0.014 kg/s flowrate.	Fin and without fin in the range 2.61–2.86 % and 2.32–2.50 % respectively.	Turkey	2021	Çiftçi et al. (2021)
Usage of TiO_2-water nanofluid through the rectangular channel underneath the PV panel.	13.80 %	37.51 %	12.68 % for PVT than 11.80 % for PV.	Algeria	2021	Ould-Lahoucine et al. (2021)
Usage of coolant fluids (pure water, 100 % ethylene glycol (EG), mixture with EG (50 %) and water) integrated with PCM with glazed unglazed PVT system.	Maximum average 14.17 % and 13.40 % of efficiency for pure water-based unglazed and glazed system.	Maximum average 71.29 % and 74.17 % of efficiency for pure water-based unglazed and glazed system.	Maximum overall 14.12 % and 13.75 % of efficiency for pure water-based unglazed and glazed system.	Iran	2020	Kazemian et al. (2020)
Utilization of concentrated photovoltaic (CPV) panel for cooling and electricity generation purposes.	10 % with CPV.	Approximately 5 %.	Efficiency improvement from 11 % to 16 % for CPV system.	Turkey	2019	Zuhur et al. (2019)
Usage of Lauric acid as PCM in aluminum container around the flow channel with 0.50–4 LPM.	11.08 % for PVT/PCM and 9.88 % for PV at 4 LPM.	Maximum 87.72 % for PVT/PCM at 2 LPM.	12.19 % for PVT/PCM and 7.09 % for PV at 0.50 LPM.	Malaysia	2019	Hossain et al. (2019)
Utilization of Ag/water nano-fluid (2 % and 4 % concentration) and water-based PVT system and evaluation of the performance for laminar, transient, and turbulent flow regimes.	14 % enhancement in efficiency for 4 wt % Ag/water nanofluid (at turbulent flow) than water-based PVT system.	Similar improvement as electrical efficiency for 4 wt % Ag/water nanofluid (at turbulent flow) than water-based PVT system.	50 % improvement in efficiency for 4 wt % Ag/water nanofluid (at turbulent flow) than water-based PVT system.	Iran	2018	Aberoumand et al. (2018)
Incorporation of ZnO/water nano-fluid along with paraffin wax as PCM underneath the PV panel and compared with PV and PVT system.	Maximum 14.05 % efficiency for NPVT/PCM system than 13.44 % and 12.56 % for NPVT and PV respectively.	Maximum 51.66 % efficiency for NPVT/PCM system than 39.86 % for NPVT.	Maximum overall exergy efficiency approximately 13.61 % than other two systems.	Iran	2018	Hosseinzadeh et al. (2018)

PCM system achieved the maximum electrical efficiency of almost 13 %. Furthermore, when PV-NePCM systems underwent testing outdoors with a chemical mixture of GNP-CuO 3 wt %, the operating temperature of the PV surface decreased by 6.6 °C and the amount of energy generated increased by 3 % as compared to the pure-PCM heat sink. Moreover, ZnO nanoparticles have better and promising thermophysical properties than the majority of other metal oxide nanoparticles available, as shown in Table 5. In order to enhance the thermophysical properties of PCM and improve the thermal and electrical power output from modified PV setups, authors plan to hybridize the PCM with Al_2O_3 and ZnO nanoparticles. As per authors' knowledge there is not a single paper available that represents the hybridization of paraffin wax with

Al_2O_3 and ZnO nano particles. This work is an upgradation of the works that are previously conducted focuses on incorporating separately Al_2O_3 and ZnO nano-particles with PCM (Chaichan and Kazem, 2018; Manigandan and Kumar, 2019).

Besides, most of the studies assessed the thermal regulation of the PV panel on an energy basis but few studies on an exergy basis including usage of nano-fluid can be found (Hosseinzadeh et al., 2018). The assessment of energy, exergy, exergoeconomic, and enviroeconomic analysis, cost analysis, energy payback time, Energy production factor analysis, life-cycle conversion efficiency, sustainability index analysis altogether in a single study using PVT/HNPCM is rare. Hence, this current study evaluates the performance of the PVT/HNPCM system for the thermal regulation of PV panels based on energy, exergy, exergoeconomic, and enviroeconomic perspectives. This experimental paper highlights the following works which present the novelty from the authors' view of survey:

- Incorporating 2.0 wt % Al_2O_3 nano-particles with PCM enhances the thermal conductivity only 12.50 % (Bayat et al., 2018) and 14.08 % (Chaichan and Kazem, 2018) Additionally, if the concentration of nanoparticles in the paraffin wax is increased, the dynamic viscosity of the paraffin wax rises dramatically. An increase in viscosity leads to a decrease in thermal conductivity (Eanest Jebasingh and Valan Arasu, 2020). Because more viscous material restricts the passage of heat transport and lowers its ability to transport thermal energy. Thus, the authors planned to restrict the total concentration of nanoparticles to 4 % (2.0 wt % of Al_2O_3 and ZnO each), in order to ensure adequate dispersion and not to reduce the latent heat of the HNPCM in significant amount.
- Three setups are designed including a conventional PV panel, PVT with PCM (PVT/PCM) and PVT with hybrid nano-PCM (PVT/HNPCM). Within PCM there is a serpentine copper pipe pattern of 270 cm in length and 6.35 mm in diameter through which water flows at constant flow rate to extract heat. Therefore, to estimate the system's heat flow, temperature gradient, and distribution, as well as the heat exchanged between the layers and its surroundings thermal network is proposed.
- Using energy, exergy, exergoeconomic and enviroeconomic analyses, the effectiveness of all three PV setups were examined in this study. The results were compared among three setups and included useable energy and useful exergy produced, energy and exergy efficiency, average cost per unit of useful exergy produced, energy payback time, energy production factor, their lifecycle conversion efficiencies, average environmental effect per unit of useful exergy produced and sustainability index.
- The most significant results from the current investigation have been compared to those from past studies that have been reported in the literature in order to keep things in perspective. This comparison was based on similarities in modification and also with the previous studies utilizing single Al_2O_3 and ZnO nano-particles and their corresponding improvements, which supports the potential ability of the system suggested in the current study.

2. Methodology

The system description and specifications, suggested setups and their explanations, the hybrid nano-PCM fabrication procedure, and the hybrid nano-PCM characterization using samples are all included in this part.

2.1. System description and specifications

In Fig. 1, the conceptual design of this experiment is shown. In this procedure, solar energy is transformed into a useable form using a 20 W polycrystalline photovoltaic panel. For the experiment, three 20 W polycrystalline photovoltaic panels were employed to transform solar energy into a useable form after being based on the results of testing four 20 W polycrystalline PV modules for consistency of power production. Table 2 lists the particular technical specifications of the used PV panels. The measurement of the inlet and outlet temperature of the working fluid (water) is carried out by using a thermocouple (MASTECH MS6514). To measure the temperature of the PV panel, a rectangular box is put behind the PV panel and contains a microcontroller (Table 4 specifications) and a programmable temperature sensor (Table 3 specifications). To measure the temperature of the PCM and HNPCM for the second and third setup, as illustrated in Fig. 2, two additional programmable sensors were mounted at the back of the PV panel and in the center of the PCM's container box. The short circuit current of the PV

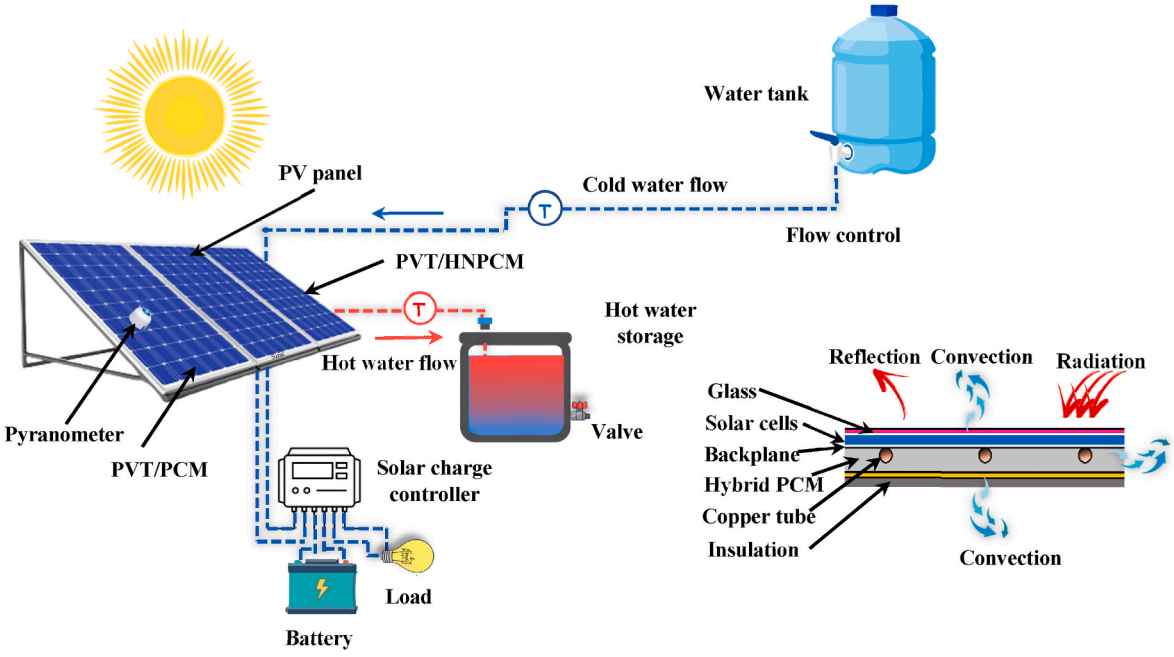

Fig. 1. Schematic layout of the experimental setup.

Table 2
Specifications of photovoltaic panel.

Brand	Generic solar panel
Type	Polycrystalline
Model	POLY-20 W
Dimension	490 mm × 350 mm× 25 mm
Rated max. power (P_{max})	20 W
Tolerance	±3 %
Rated current (I_{mp})	1.15 A
Rated voltage (V_{mp})	17.40 V
Open circuit voltage (V_{oc})	22.40 V
Short circuit current (I_{sc})	1.23 A
Weight	1.30 kg
STC	1000 W/m^2, AM 1.5, 25 °C

Table 3
Specification of programmable sensor.

Parameters	Values
Model	Dsb18b20
Operating voltage	3–5 V
Temperature range	−55 °C to +125 °C
Output resolution	9-12 bit
Accuracy	±0.50 °C
Conversion time	750 ms at 12 bit

panel is measured using a digital multimeter, and solar irradiance is gauged using a pyranometer (Hukseflux LP02-LI19). Through two holes that had been drilled into the top of the container, hybrid nano PCM was poured into the housing. Additionally serving as a breather to keep the pressure from rising, these perforations served their purpose. The amount of PCM was calculated using a number of factors, including the melting point temperature, energy storage capability, thermal conductivity, and predicted sunlight intensity of the PCM. According to the calculations and evaluation of those factors, 2 kg of PCM was determined to be the ideal quantity for complete melting. The PCM container made of plastic wood is sealed tightly with a serpentine copper tube that has a flawless connection between the PV panel and pipe shown in Fig. 2 and kg of paraffin wax (specified in Table 5) with hybrid nano-particles that have an identical content of 2.0 wt % Al_2O_3 and ZnO. The PVT system uses thermal energy storage to store the thermal energy for household uses.

2.2. Experimental setup

The experiments were performed at Rajshahi University of Engineering and Technology, RUET campus, Rajshahi (latitude: 24°22′N, longitude: 88°36′E), Bangladesh as shown in Fig. 2. The studies were placed on days with sunshine and a cool breeze, and the intensity of the solar radiation ranged from 300 W/m^2 to 850 W/m^2. Around 26 °C was the temperature in the room or ambient. Using a water tap coupled to an above tank, the pipeline's water flow rate was maintained at 0.0021 kg/s to extract heat from the PCM and HNPCM. A flow rate sensor was used to measure the flow rate. Three different scenarios have been explored in this experimentation technique, including (i) a PV panel (only photovoltaic panel), (ii) a PVT/PCM system with a water-flowing fluid, and (iii) a PVT/hybrid nano-PCM (PVT/HNPCM, 2.0 wt % Al_2O_3, and 2.0 wt % ZnO) system.

Table 4
Specification of microcontroller.

Parameters	Values
Model	NodeMCU ESP8266
Operating voltage	3.30 V
Temperature range	−40 °C to +125 °C
Size	58 mm × 32 mm

Table 5
Thermo-physical characteristics of paraffin wax and nano-particles (Fayaz et al., 2019).

Thermo-physical Properties	Paraffin wax	Al_2O_3 nano particles	ZnO nano particles
Thermal conductivity	0.18 W/m K	17.65 W/m K	23.4 W/m K
Density	805 kg/m^3	3970 kg/m^3	5606 kg/m^3
Particle size	–	30–35 nm	40–50 nm
Specific heat	2150 J/kg K	525 J/kg K	514 J/kg K
Volume expansion	12.50 %	–	
Particle shape	–	Spherical	Spherical
Purity	–	+99 %	+99 %
Temperature of transition	44 °C	–	–
Transitional interval	1 °C	–	–
Latent heat	−242 kJ	–	–

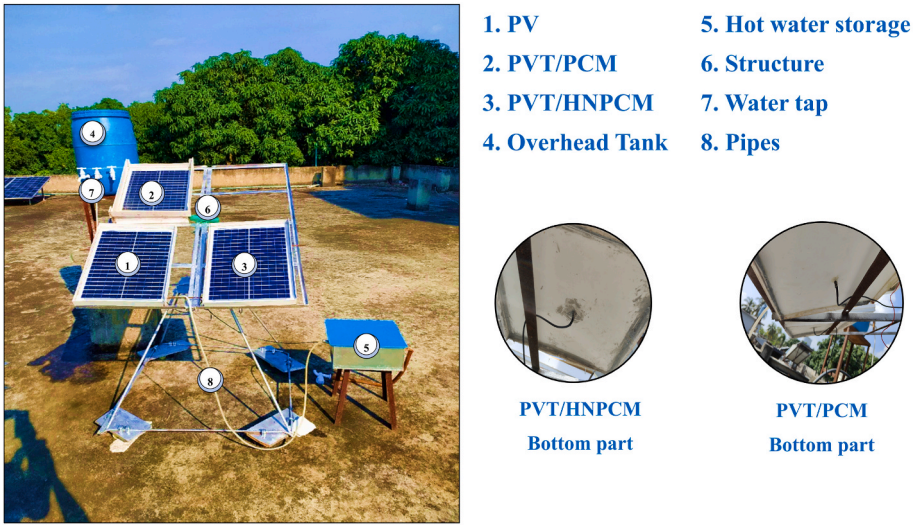

Fig. 2. Experimental setup of PVT hybrid nano-PCM (PVT/HNPCM) system.

2.3. Fabrication of the hybrid nano-PCM

Using a two-step process, hybrid nano-PCM was prepared by dispersing nanoparticles into PCM. During this procedure, the digital weighing equipment was used to weigh the nanoparticles and paraffin wax in the appropriate amounts. The measured paraffin wax was then melted in a beaker at 70 °C, and nano-additives (Al_2O_3 and ZnO) were added at the identical 2.0 wt % concentration. The wax was then agitated at 70 °C for around 2 h using a stirring machine at 800 rpm. The beaker was then placed in an ultrasonic vibration machine operating at a frequency of 33 kHz for about an hour to ensure appropriate dispersion of nanoparticles into PCM. The sample was finally cooled to room temperature. The schematic diagram of the two-step preparation method is shown in Fig. 3. In 2 kg of paraffin wax, 2.0 wt % each of aluminum oxide (20 nm) and zinc oxide (50 nm) nanoparticles are included. The hybrid nano-PCM is introduced and sealed after a serpentine copper pipe is put on the PV panel's rear side. After being sonicated in the ultrasonic bath, the mixture was put to the panel. Fig. 4 displays a hybrid nano-PCM with a serpentine copper tube.

2.4. Characterization of hybrid nano-PCM

The Fourier transform infrared spectrum (FTIR) of the hybrid PCM/hybrid nanocomposites is calculated using a PerkinElmer Spectrum Two-UATR. Spectra are detected by the MIR TGS's integrated detector (15,000-370 cm^{-1}). A scan at a speed of 0.20 cm^{-1} covered the ideal scan range of 7800-450 cm^{-1}. This investigation is important to understand the chemical interactions between nano-ZnO, nano-Al_2O_3, and paraffin. In general, ZnO and Al_2O_3 nanoparticles should be finely disseminated inside the paraffin framework rather than reacting with the paraffin for best results. On a Zeiss (EVO-18) SEM, measurements of the morphology and size of the materials were made using Scanning Electron Microscopy. Al_2O_3 and ZnO nanoparticles in the PCM composite matrix are employed as the basis material, and SEM micrographs are used to analyze the size, shape, and dispersion of the nanomaterials within the base material. The samples received a gold covering to avoid charge buildup and an in-lens detector to reveal the samples' surface composition. Using the PerkinElmer TGA 4,000, TGA analysis was used to assess the thermal stability of pure commercial grade PCM (paraffin) and hybrid PCM/ZnO–Al_2O_3 nanocomposites. The samples were tested at a gas pressure of 2.60 bar and an ultra-high pure nitrogen gas flow rate of 19.80 mL/min. Using a thermal conductivity tester DTC-25 with a thermal conductivity range of 0.1–20 W/m K and accuracy ranging from 3 % to 8 % depending on conductivity, the thermal conductivity of PCM and hybrid nano/PCM was measured. Depending on heat resistance, the specimen's thickness can reach a maximum of 1.25" (32 mm), and thin films as thin as 0.004" (0.1 mm) are supported. On the paraffin wax samples, a differential scanning calorimetry (DSC) examination was done. In order to determine the heat capacity, latent heat of fusion, and melting temperature of the hybrid nano-PCM samples, a differential scanning calorimeter (Mettler-Toledo DSC822) is employed. About 15–20 mg of material is placed into the DSC cell, and nitrogen is always used as the purge gas. Three samples are put into crucibles without being taken out of the measuring crucible, and they are analyzed consecutively through a number of heating/cooling cycles.

3. Mathematical expressions for determining efficiency

In this varied section, numerical equations are presented to assess the performance of the suggested systems. Among them are energy and exergy efficiency, environmental analysis, sustainability index, energy production factor (EPF), energy payback time (EPBT), exergoeconomic analysis, life cycle conversion efficiency (LCCE), and uncertainty estimation. It is assumed that the system operates in a steady-state environment and that thermal characteristics, including specific heat, thermal conductivity, and latent heat, remain constant. Furthermore, other variables such as the quantity of water vapor in the air, wind speed, and the percentage of cloud cover in the sky were not taken into account.

3.1. Energy efficiency

The computation of the electrical power can be done by applying the following relation, where $V_{oc} = 21.50$ V and $I_{sc} = 1.67$ A are the open circuit voltage and short circuit current of the PV module. The output electrical power can be calculated by the following equation (Li et al., 2022):

$$\dot{E}_{el} = V_{oc} \times I_{sc} \times FF \quad (1)$$

Where, V_{oc}, I_{sc}, and FF refer to the open circuit voltage, short circuit

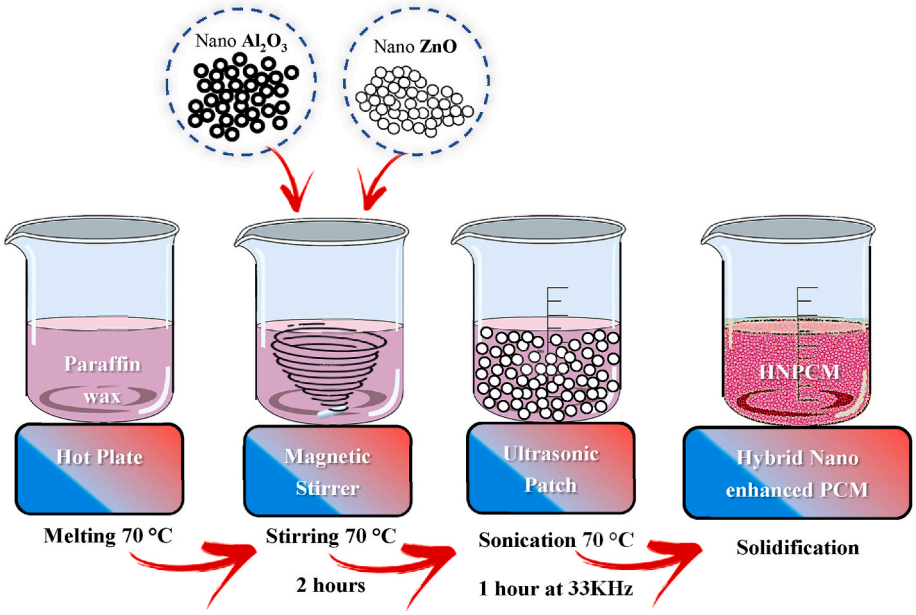

Fig. 3. Schematic diagram of two-step preparation method.

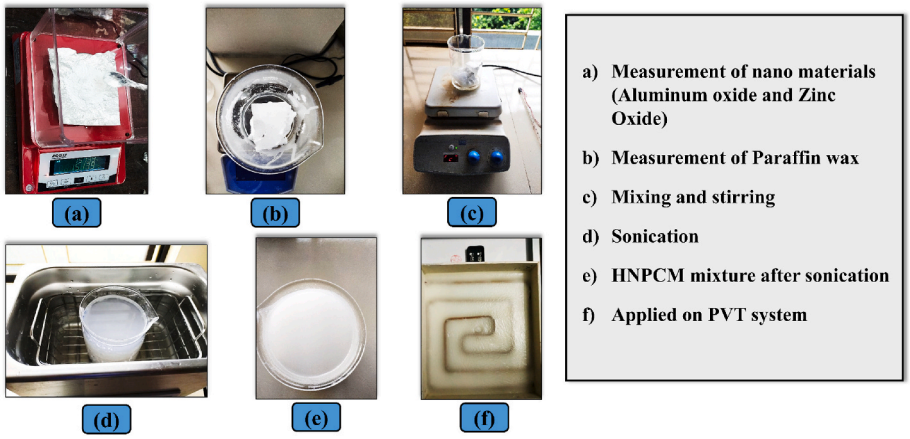

Fig. 4. Final preparation process for fabrication PVT system.

current and fill factor.

The expression for fill factor (FF) can be written as follows (Li et al., 2022):

$$FF = \frac{V_{max} \times I_{max}}{V_{oc} \times I_{sc}} \tag{2}$$

The expression for the solar irradiation of the system can be obtained as follows (Li et al., 2022):

$$\dot{E}_{sun} = \ddot{G} \times A_c \times \dot{\tau}_g \times \alpha_{cell} \tag{3}$$

Where, $\ddot{G}$ indicates to the rate of solar irradiation, A_c the solar panel area, τ_g the glass transmissivity, and α_{cell} the PV panel cell absorptivity.

The electrical efficiency is defined as the ratio of electrical power to the sun irradiation and expressed as follows (Li et al., 2022):

$$\eta_{el} = \frac{\dot{E}_{el}}{\dot{E}_{sun}} = \frac{V_{oc} \times I_{sc} \times FF}{\dot{G} \times A_c \times \dot{\tau}_g \times \alpha_{cell}} \tag{4}$$

The thermal power can be computed from the following formula (Li et al., 2022):

$$\dot{E}_{th} = \dot{m} \times C_{p,f} \times \left(T_{f,out} - T_{f,in}\right) \tag{5}$$

Where, $\dot{m}$ is the mass flow rate of the coolant, $C_{p,f}$ the specific heat of the coolant, $T_{f,out}$ and $T_{f,in}$ the outlet and inlet temperature of the coolant respectively.

The thermal efficiency of the system can be defined as the ratio of thermal power to the sun irradiation and can be obtained from the following expression (Yazdanifard et al., 2020):

$$\eta_{th} = \frac{\dot{E}_{th}}{\dot{E}_{sun}} = \frac{\dot{m} \times C_{p,f} \times \left(T_{f,out} - T_{f,in}\right)}{\dot{G} \times A_c \times \tau_g \times \alpha_{cell}} \tag{6}$$

The overall efficiency of the system is the sum of the electrical efficiency and thermal efficiency and can be obtained as follows (Yazdanifard et al., 2020):

$$\eta_{ov} = \eta_{el} + \eta_{th} \tag{7}$$

3.2. Exergy efficiency

The analysis of exergy is completely identical to the energy analysis. PVT/PCM and PVT/HNPCM are considered as a control volume and assuming a steady state condition, the exergy balance for the system is written as follows (Sardarabadi et al., 2017a):

$$\sum \dot{E}x_{in} = \sum \dot{E}x_{out} + \sum \dot{E}x_{loss} \tag{8}$$

$$\dot{E}x_{sun} + \dot{E}x_{mass,in} = \dot{E}x_{el} + \dot{E}x_{mass,out} + \dot{E}x_{loss} \tag{9}$$

Where, $\dot{E}x_{in}$, $\dot{E}x_{out}$, and $\dot{E}x_{loss}$ indicates the rate of exergy input, output, and loss.

Sun exergy is calculated by using the following formula (Park et al., 2014):

$$\dot{E}x_{sun} = \dot{G}\left(1 - \frac{T_{amb}}{T_{sun}}\right) \tag{10}$$

Where, T_{amb} and T_{sun} represent the ambient and sun temperature (T_{sun} = 5800 K) respectively.

The output electrical energy is regarded as the useful available energy. So, the electrical energy is equal to the electrical exergy, given as follows (Chow et al., 2009):

$$\dot{E}x_{el} = \dot{E}_{el} \tag{11}$$

The thermal exergy of the system can be obtained from the following relation (Sardarabadi et al., 2017a):

$$\dot{E}x_{th} = \dot{m}_f.C_{p,f}\left[\left(T_{f,out} - T_{f,in}\right) - T_{amb}\ln\left(\frac{T_{f,out}}{T_{f,in}}\right)\right] \tag{12}$$

Where, $\dot{m}_f$, $C_{p,f}$, $T_{f,out}$, $T_{f,in}$ refers to the mass flow rate, specific heat, outlet, and inlet temperature of the flowing coolant respectively.

Total exergy for the system can be attained as follows (Sardarabadi et al., 2017a):

$$\dot{E}x_{total} = \dot{E}x_{el} + \dot{E}x_{th} \tag{13}$$

Identical to the energy analysis, the system electrical and thermal exergy efficiency can be defined as the ratio of the output electrical and thermal exergy respectively, to the sun exergy. Hence, the electrical and thermal exergy efficiency can be presented as follows (Sardarabadi et al., 2017a):

$$\varepsilon_{el} = \frac{\dot{E}x_{el}}{\dot{E}x_{sun}} = \frac{\dot{E}_{el}}{\dot{G}\left(1 - \frac{T_{amb}}{T_{sun}}\right)} = \frac{V_{oc} \times I_{sc} \times FF}{\dot{G}\left(1 - \frac{T_{amb}}{T_{sun}}\right)} \tag{14}$$

$$\varepsilon_{th} = \frac{\dot{E}x_{th}}{\dot{E}x_{sun}} = \frac{\dot{m}_f.C_{p,f}\left[\left(T_{f,out} - T_{f,in}\right) - T_{amb}\ln\left(\frac{T_{f,out}}{T_{f,in}}\right)\right]}{\dot{G}\left(1 - \frac{T_{amb}}{T_{sun}}\right)} \tag{15}$$

Overall exergy efficiency can be defined as the ratio of total exergy output to the sun exergy, expressed as follows (Chow et al., 2009):

$$\varepsilon_{ov} = \frac{\dot{E}x_{el} + \dot{E}x_{th}}{\dot{E}x_{sun}} \tag{16}$$

3.3. Economic analysis

The first target is to decrease the electricity production cost for per unit (kWh). The expression of first annual cost (FAC) is given below (Esfahani et al., 2011):

$$FAC = CRF \times P \tag{17}$$

Where, *CRF* and *P* refers the capital recovery factor and capital cost of the PV panel.

The expression of CRF is written as follows (Hassan et al., 2021):

$$CRF = \frac{i(1+i)^n}{(1+i)^n - 1} \tag{18}$$

Where, *i* stands for interest rate and *n* stands for the lifespan of the panel.

The annual salvage value of the panel is written as follows (Yousef and Hassan, 2019):

$$ASV = S \times SFF \tag{19}$$

Where, *S* and *SFF* stand for the salvage value and sinking fund factors respectively.

The *SFF* can be computed as (Yousef and Hassan, 2019):

$$SSF = \frac{i}{(1+i)^n - 1} \tag{20}$$

The annual maintenance cost (AMC) is considered as the 15 % of the FAC (Yousef and Hassan, 2019):

$$AMC = 0.15 \times FAC \tag{21}$$

Annual cost (AC) can be calculated as below (Yousef and Hassan, 2019):

$$AC = FAC + AMC - ASV \tag{22}$$

The cost of DC electricity in $/kWh can be computed as (Yousef and Hassan, 2019):

$$C_e = \frac{AC}{En_{annual}} \tag{23}$$

3.4. Energy payback time (EPBT)

Energy payback time (EPBT) is defined as the required time to recover the energy invested into the system. The invested energy indicates the total amount of energy spent from the manufacture level to the entire life of the equipment which is incorporated with embodied energy ($E_{a,in}$). The EPBT should be kept as short as possible for the system. It can be computed from the view of energy as well as exergy (Abo-Elfadl et al., 2021):

$$(EPBT)_{en} = \frac{E_{a,in}}{En_{out}} \tag{24}$$

$$(EPBT)_{ex} = \frac{E_{a,in}}{Ex_{out}} \tag{24}$$

3.5. Energy production factor (EPF)

Energy production factor (EPF) of a system is a parameter to judge the performance. It is the reciprocal of EPBT and this value will be unity only if the value of EPBT is unity. The value of EPF should be more than unity and should be kept as high as possible for the system for cost effective. The expression is given below (Tiwari and Tiwari, 2016):

$$(EPF)_{ex} = \frac{Ex_{out}}{E_{a,in}} \tag{26}$$

Or,

$$(EPF)_{ex} = \frac{1}{(EPBT)_{ex}} \tag{27}$$

If the entire life of the system is considered, then the equation would be as follows (Tiwari and Tiwari, 2016):

$$(EPF)_{ex} = L\frac{Ex_{out}}{E_{a,in}} \tag{28}$$

Where, L is the life of the system.

3.6. Life cycle conversion efficiency (LCCE)

The life cycle conversion efficiency (LCCE) is concerned with decreasing environmental consequences by enabling increased solar PVT performance. The LCCE can be defined as the ratio of net system output to the solar input received by the system throughout its lifetime. The higher LCCE value of PVT system demonstrates its strong environmental friendliness. The expression in the exergy view is given as follows (Tiwari and Tiwari, 2016):

$$(LCCE)_{ex} = \frac{Ex_{out} \times L - E_{a,in}}{E_{sol}\, L} \tag{29}$$

Where, E_{sol} refers to the annual solar energy.

3.7. Exergoeconomic analysis

Exergoeconomic is another approach to make a relation between the cost of the system with the obtaining exergy output. It is defined as the ratio of the exergy out to the annual cost of the system. It is indicated exergy gain (kwh) per unit cost. The value of Exergoeconomic should be high as possible from the system. The expression for the Exergoeconomic parameter (R_{ex}) is given below (Yousef and Hassan, 2020):

$$R_{ex} = \frac{Ex_{out}}{AC} \tag{30}$$

3.8. Environmental analysis

Fossil fuel-based technology for energy production can emit a large amount of greenhouse gas to the environment whereas the PV technology is considered as the most potential for generating electricity as well as for mitigating the greenhouse gas emission. Therefore, environmental analysis has been conducted to analyze the ecological friendly behavior of the PV technology over the other technologies.

The annual reduction of carbon emission has been calculated by the following formula (Deniz and Çınar, 2016):

$$\varphi_{co_2} = \frac{En_{out} \times n \times \alpha_{co_2}}{1000} \tag{31}$$

Where, φ_{co_2}, α_{co_2}, *n*, and En_{out} represent environmental parameter, conversion factor (kg/kWh), number of years, annual energy output (kWh) respectively.

The earned carbon credit expression is given below (Elbar et al., 2019):

$$Z_{co_2} = z_{co_2} \times \varphi_{co_2} \tag{32}$$

Where, Z_{co_2}, and z_{co_2} refer to the enviro-economic parameter and global carbon value which is taken as 14.5 $ per ton of CO_2 (Hassan et al., 2020; Yousef et al., 2019).

3.9. Sustainability index

Sustainability analyses aim to ensure the effective use of various resources. The sustainability index (SI) technique, which is directly tied to exergy efficiency, is used for this assessment (Abdo et al., 2021). The efficiency of energy conversion, greenhouse gas emissions during the technical life cycle, the cost of electricity generation, the intensity of solar radiation throughout the year, the location of installation requirements, and the social impacts are just a few of the many variables that can be used to evaluate the sustainability index of solar cell systems. Photovoltaic thermal exergy rate (ψ) can be defined as (Wahab et al., 2020):

$$\psi = \frac{\dot{E}x_{overall}}{\dot{E}x_{solar,in}} \tag{33}$$

Sustainability index can be calculated as follows (Wahab et al., 2020):

$$SI = \frac{1}{1-\psi} \tag{34}$$

The value of SI is in the ranges between 1 and ∞. From equation (34), it is clearly evident that the zero exergy means the SI value is 1, which is the lowest value of SI. Therefore, the higher the exergy efficiency larger the sustainability index i.e. the better utilization of available energy resources.

3.10. Uncertainty estimation

The uncertainties of the experimental setup were identified and expressed in a manner that complies with the literature (Gelis et al., 2022).

The partial derivative of the sensitivity is written as

$$\frac{U_R}{R} = \sqrt{\left(\frac{X_n \partial R}{R \partial X_n}\right)^2 \frac{U_{X_n}^2}{X_n^2}} \tag{35}$$

R is considered as the resultant of all uncertainty, R═R (X1, X2⋯⋯X_n) (Gelis et al., 2022)

$$WRi = \left[\left(\frac{\partial R}{\partial x_1} w_1\right)^2 + \left(\frac{\partial R}{\partial x_2} w_2\right)^2 + \ldots + \left(\frac{\partial R}{\partial x_n} w_n\right)^2\right]^{\frac{1}{2}} \tag{36}$$

The cumulative uncertainties of the systems during a period of experimentation were discovered to be less than 3 %, which is within a reasonable range. Cloud cover and humidity have an impact on how well a PV panel performs. The current and voltage decreased as a result of the high humidity levels. The average relative humidity during the research period was under 60 %. Additionally, additional factors including the amount of air water vapor, the speed of the wind, and the proportion of the sky covered in clouds were not taken into consideration.

4. Results and discussions

Based on a variety of test results, the properties of hybrid nano-PCM are examined in this section. For the improved PVT/HNPCM system, a thermal heat transfer network is also presented. Additionally, each system undergoes a comprehensive analysis of its cell temperature variation, electrical efficiency, thermal efficiency, overall efficiency, energy efficiency, environmental, economical, and sustainable aspects.

4.1. Property analysis: hybrid nano-PCM

The thermophysical properties of the sample were observed by undergoing some tests including SEM, DSC, TGA, FTIR analysis, and thermal conductivity analysis. The FTIR test was performed using A PerkinElmer Spectrum Two-UATR to investigate the chemical interaction of nano-particles inside the base PCM but there is no distinct peak indicating better blending without any chemical reaction, shown in Fig. 5. Spray drying, precipitation techniques, two step method and sol-gel synthesis are a few examples of reliable and effective synthesis processes. For instance, employing a synthesis technique mentioned above guarantees improved nanoparticle dispersion in the PCM matrix may provide a more stable NePCM. With precisely controlled of these techniques provide over the size, shape, and composition of the nano-particles, it can result in a more stable NePCM with improved durability over multiple thermal cycles (Tariq et al., 2020). The morphology of the nano-particles inside the base material (PCM) was observed using SEM imaging and exhibited stronger physical contact of nano-particles with PCM without having significant agglomeration, shown in Fig. 6. This indicates that nano-particles will retain thermal stability and uniform distribution over various charging and discharging cycles. PerkinElmer TGA 4000 analyzer was used and 12 mg of sample was kept at the heating rate 20 °C/min in the range of temperature varying from 30 °C to 800 °C. 2.0 wt % of hybrid nano-particles exhibited rapid degradation and lower thermal stability at a lower temperature range due to having a higher thermal conductivity, shown in Fig. 7(a). The measurement of heat capacity, latent heat of fusion, and the melting point temperature of the hybrid nano/PCM was done using DSC. 15–20 mg amount of the sample was filled in a DSC cell and a heating/cooling cycle was performed on the sample. 2.0 wt % of HNPCM showed lower melting temperature by around 60.07 °C as well as latent heat of fusion by around 228.93 kJ/kg compared to others due to its higher thermal conductivity, shown in Fig. 7(b). The thermal conductivity property was examined using thermal conductivity tester DTC-25 and the accuracy of the tester was about ±3 %–8 %. The thickness of the sample was kept at 32 mm for the testing and the testing result exhibited a maximum 41.56 % improvement in thermal conductivity of 2.0 wt % of HNPCM than other samples, shown in Fig. 7(c).

4.2. Thermal heat transfer network

The solar energy is harnessed by using photovoltaic panel into electricity. Heat transfer into the PVT/HNPCM system generally takes place by conduction, convection, and radiation. At first, the solar energy strikes the surface of the PV panel. A portion of the solar energy is lost to the environment through convection and radiation, a portion is converted into the useful form of electrical energy, and the remaining portion is absorbed by the PV panel. The absorbed portion is transferred to the rear part of the PV panel where heat is conveyed through the hybrid nano-PCM layers by conduction. The hybrid nano-PCM layers get melted and transfers heat to the copper tube by conduction to water through convection, then the heat is conducted by the plastic wood box which is considered as the lowest part of the system. Finally, the heat is dissipated to the environment by natural convection and radiation. Fig. 8 shows the flow of heat through the system by different modes.

4.3. Variation of cell temperature

As previously said, the main purpose of using PVT/HNPCM and PVT/PCM systems is to improve the performance of the conventional PV module by cooling the solar cells. As a result, in photovoltaic systems, the temperature of the solar cells is crucial. The study's Fig. 9 demonstrates how using Al_2O_3 and ZnO with the PCM influences the surface temperature of the PVT system. The maximum cell temperatures of the PVT/HNPCM, PVT/PCM, and PV systems were 56.10 °C, 59.70 °C, and 61.50 °C, respectively, as observed under the highest solar irradiation of 826 W/m^2. As a consequence, when Al_2O_3 and ZnO were mixed with the PCM of the PVT system, the average surface temperature was lowered by 5.40 °C. Moreover, the difference between the surface temperature of the PVT/HNPCM and PVT/PCM systems was 3.60 °C.

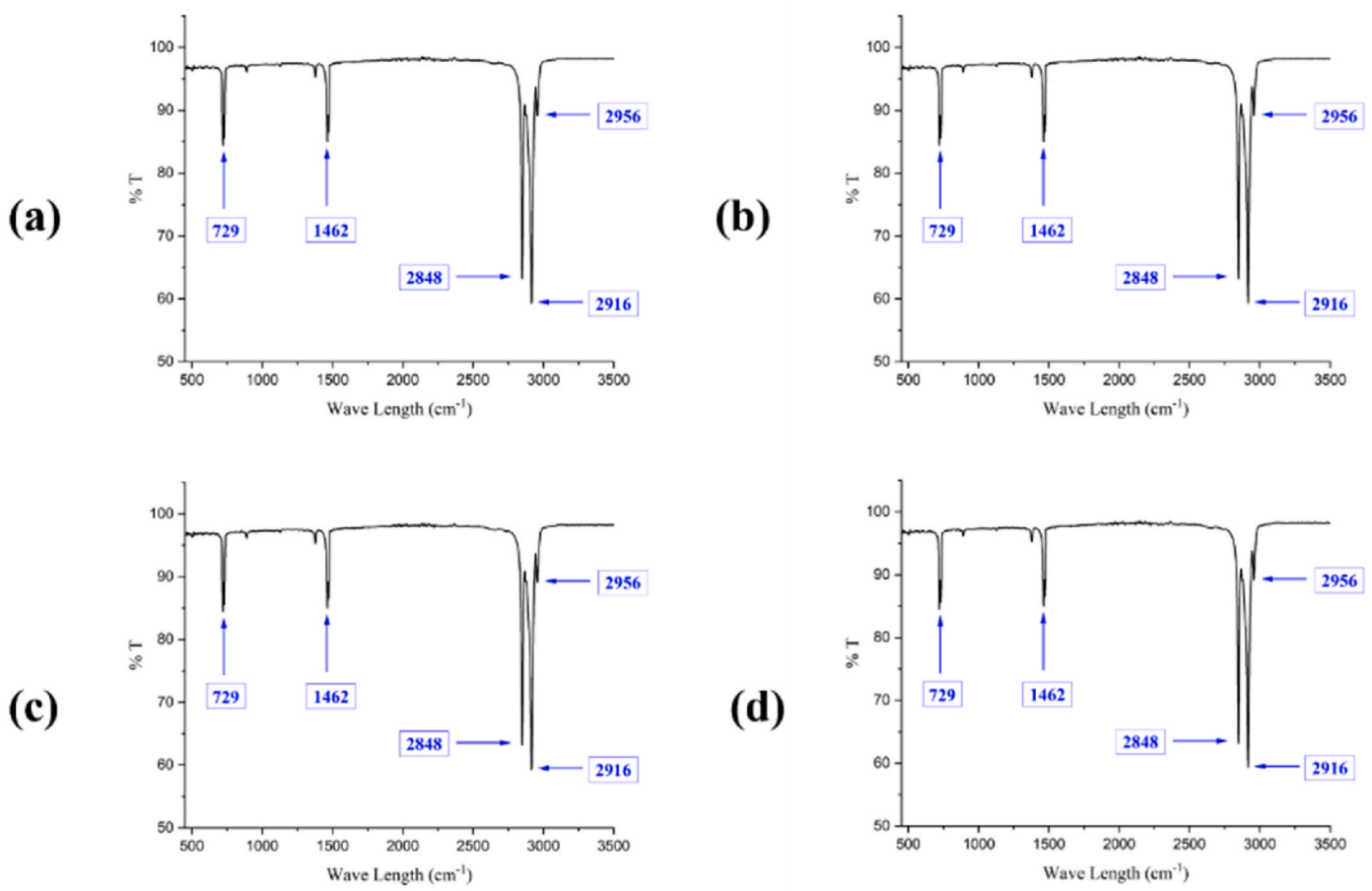

Fig. 5. FTIR results of the (a) Pure paraffin (b) 0.50 % Hybrid nano PCM (c) 1.0 wt % Hybrid nano PCM (d) 2.0 wt % Hybrid nano PCM.

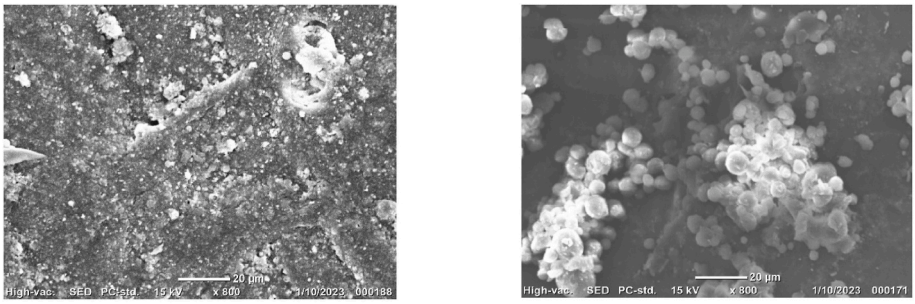

Fig. 6. SEM images of (a) 1.0 wt % Hybrid nano PCM (b) 2.0 wt % Hybrid nano PCM.

4.4. Electrical efficiency

Figs. 10 and 11 respectively depict the variation in the output electrical power, electrical efficiency, and electrical efficiencies of the PVT/PCM and PVT/HNPCM systems. It is clear from Fig. 10 that the electrical output powers of the PVT/PCM system were raised just before solar noon. This is brought on by the system's increased solar light absorption. Additionally, the maximum electrical output powers of the PVT/HNPCM system, PVT/PCM system, and PV system are 13.47 W, 13.11 W, and 9.99 W, respectively. As a result of the photovoltaic thermal system and hybrid nanomaterials being utilized in conjunction with the PCM, the maximum output electrical power is raised by almost 3.48 W (i.e., around 34.84 %). This is due to a lower surface temperature of the PVT/HNPCM system. The PVT/HNPCM system, PVT/PCM system, and PV system all have maximum electrical energy efficiency of 15.56 %, 15.15 %, and 11.54 %, respectively. Therefore, the PVT/HNPCM system's relative improvement in electrical energy efficiency over the traditional PV module is about 34.84 %. It is obvious that at the busiest times of the day, electrical power and efficiency are at their highest. Additionally, the results show that PVT/HNPCM outperforms PVT/PCM for both parameters. Additionally, it has been discovered that PVT/HNPCM has roughly 2.75 % and 2.71 % more electrical power and efficiency than PVT/PCM.

4.5. Thermal efficiency

Due to the overhead tank's height from the floor, Figs. 12 and 13 show the daily changes in thermal power and thermal efficiency of the

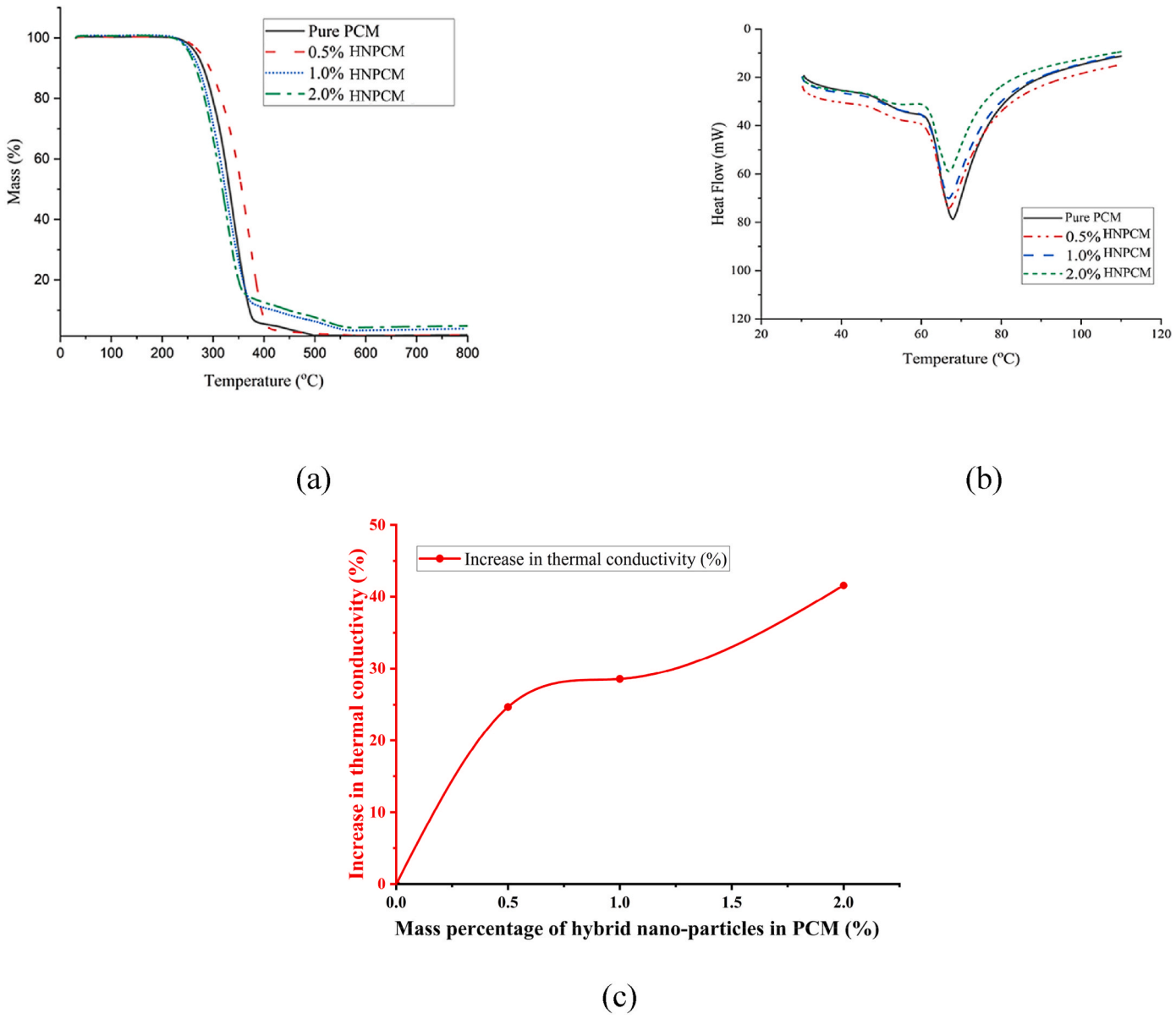

Fig. 7. (a) TGA, (b) DSC curve of pure paraffin and hybrid PCM/ZnO–Al_2O_3 nanoparticles, (c) Percentage thermal conductivity improvement with respect to increasing mass percentage of hybrid nanomaterials.

PVT/PCM and PVT/HNPCM at a uniform mass flow of 0.0021 kg/s. As a result of the hybrid nano-PCM's increased thermal conductivity, which enables a quicker rate of heat transfer to water, it has been discovered that PVT/HNPCM has a higher thermal efficiency than PVT/PCM. Thus, when the photovoltaic thermal system and hybrid nanomaterials were employed in conjunction with the PCM, the maximum output thermal power increased in comparison to the PVT/PCM system by almost 7.06 W (i.e., approximately 17.40 %). At a mass flow rate of 0.0021 kg/s, thermal efficiency is 55 % with a PVT/HNPCM system and 46.88 % with a PVT/PCM system.

4.6. Overall efficiency

Fig. 14 shows the overall effectiveness of the PVT/PCM and PVT/HNPCM for the ideal flowrate at 0.0021 kg/s throughout the day from 9 a.m. to 4 p.m. Due to the PVT/HNPCM system's better thermal conductivity and rate of heat extraction from the panel, it has been demonstrated that the addition of hybrid nanoparticles to PCM has a higher overall efficiency than PVT/PCM for any abscissa. throughout both cases, the overall efficiency increases gradually throughout the morning before falling about noon as a result of the waning sun irradiation. At 12:00 p.m., the greatest overall efficiency was discovered to be around 70.59 % for PVT/HNPCM and 62.02 % for PVT/PCM due to that day's peak solar radiation. Additionally, it is hypothesized that the PVT/HNPCM system is more efficient overall than the PVT/PCM system by about 13.82 %. The graph also shows that the PVT/HNPCM system outperforms the PVT/PCM system in terms of performance.

4.7. Exergy efficiency

From the perspective of thermodynamics, electrical energy has a higher quality of energy than thermal energy, and the qualities of equal amounts of thermal and electrical energy are not the same. Because of the temperature differences between thermal reservoirs, thermal energy cannot totally be transformed into useful work, whereas all of the electrical energy generated by solar panels can be viewed as useful work (Sardarabadi et al., 2017b). In actuality, electrical energy is crucial to the energy efficiency of PVT system. As a result, the electrical efficiency

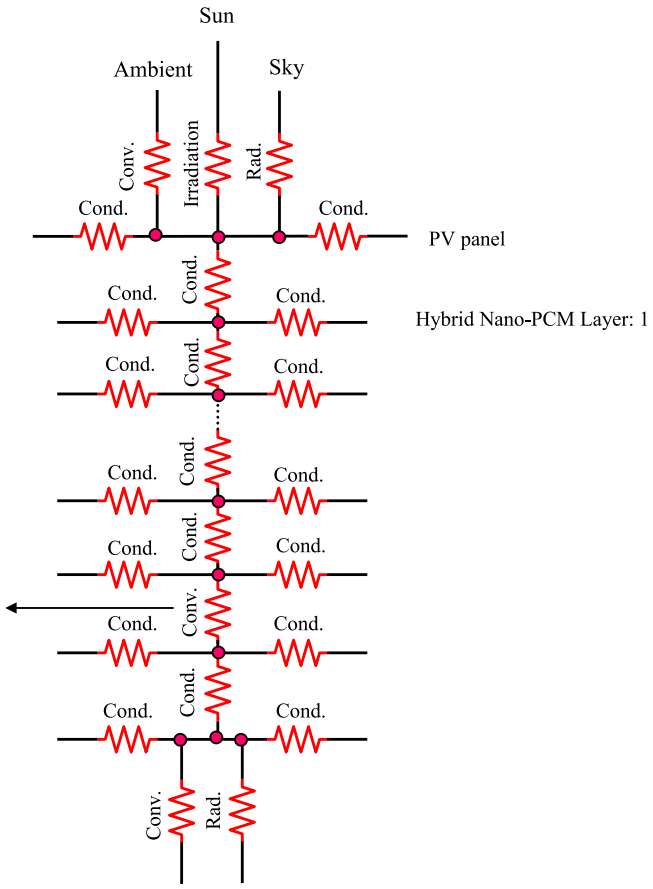

Fig. 8. Thermal network of heat flow.

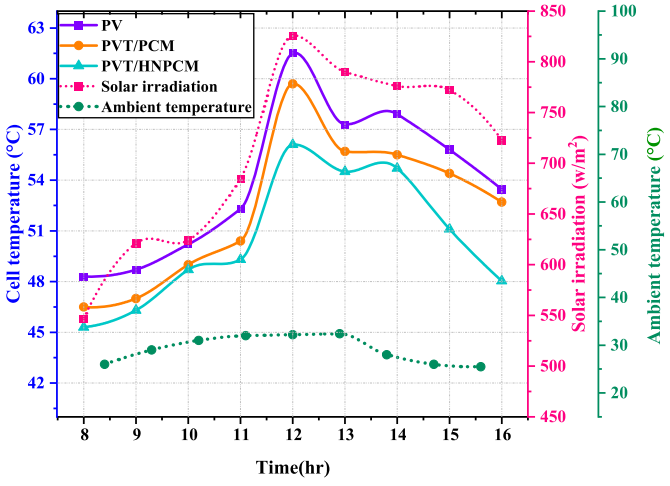

Fig. 9. Variations of the cells temperature and solar irradiance for the conventional PV module, the PVT/PCM and PVT/HNPCM systems.

and exergy efficiency follow similar trends. Additionally, exergy evaluation, which is based on the principles of thermodynamics, is necessary to evaluate the actual performance of the PVT systems because it is more accurate while taking into account the quality of each component. Figs. 16 and 18 show the exergy efficiency of the PV, PVT/PCM and PVT/HNPCM systems under similar situations. The exergy efficiency is calculated by adding its thermal and electrical exergy efficiencies (Kazemian et al., 2018). As was previously established, compared to

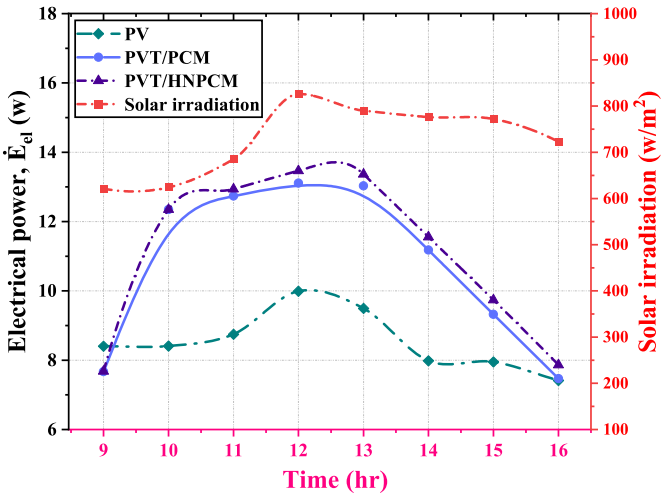

Fig. 10. Variations of output electrical power of PV, PVT/PCM, PVT/HNPCM systems.

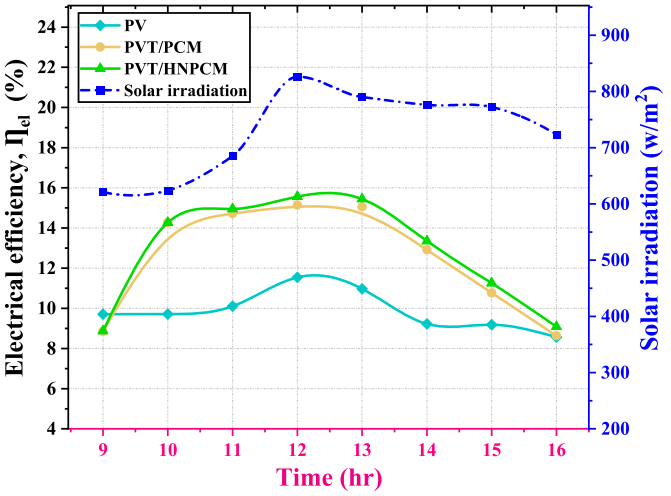

Fig. 11. Variations of output electrical efficiency of PV, PVT/PCM, PVT/HNPCM systems.

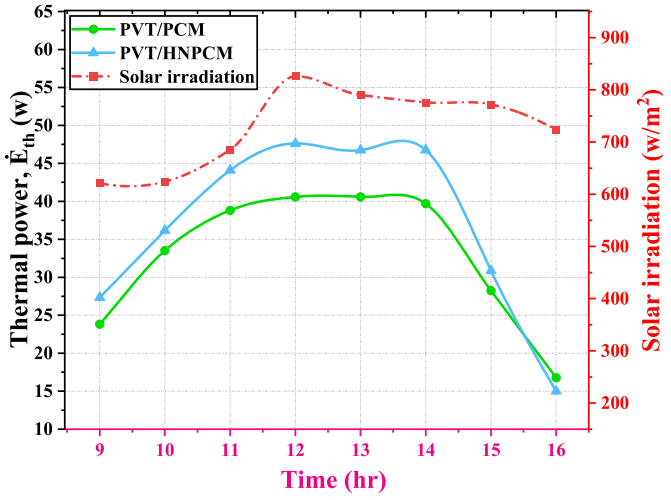

Fig. 12. Variations of output thermal power of PV, PVT/PCM, PVT/HNPCM systems.

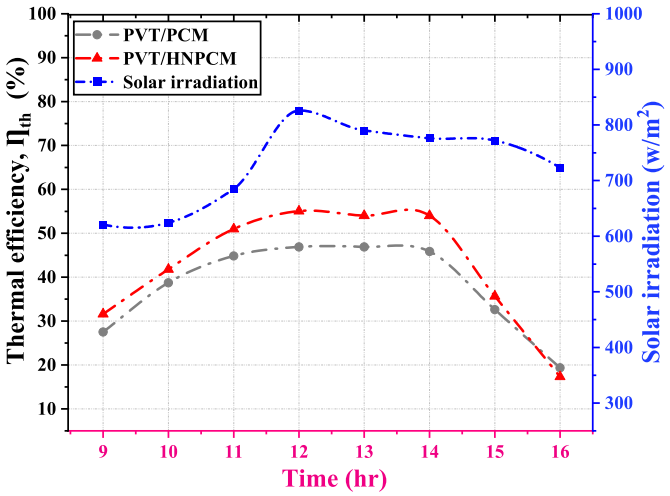

Fig. 13. Variations of output thermal efficiency of PV, PVT/PCM, PVT/HNPCM systems.

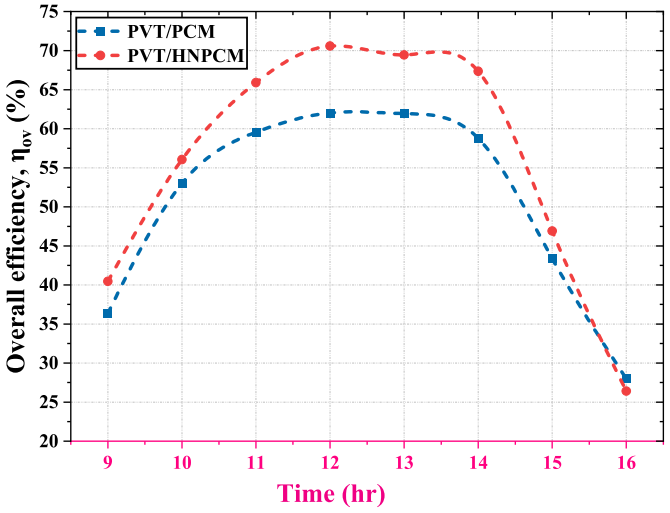

Fig. 14. Overall efficiency of PVT/PCM and PVT/HNPCM.

thermal energy (which is considered low-grade), electricity has a greater quality and is regarded high grade energy. When the photovoltaic thermal system and hybrid nanomaterials were employed in conjunction with the PCM, the maximum output electrical power increased by almost 3.48 W (i.e., around 34.84 %) due to a lower surface temperature of the PVT/HNPCM system. The PVT/HNPCM system, PVT/PCM system, and PV system all have maximum electrical exergy efficiency of 11.50 %, 11.19 %, and 8.53 %, respectively. This results in trends for energy efficiency and electrical efficiency that are comparable. In this aspect, the energy efficiency of all three setups is primarily influenced by its electrical exergy efficiency. Thus, like electrical efficiency, higher energy efficiency starts in the middle of the day reaches its lowest value at the end of the trial. Fig. 15 depicts the electrical exergy variation of the three systems and the maximum electrical exergy is attained about 13.47 W in case of PVT/HNPCM, which is comparatively higher than that of the other two. It can be seen by contrasting Figs. 20 and 21 that an implementation in nanoparticles with moderate concentration leads to an improvement in electrical exergy efficiency. Thus, from Fig. 17 the maximum output thermal exergy in comparison with PVT/PCM system is increased by nearly 0.165 W (i.e., around 29.46 %) when the photovoltaic thermal system and hybrid nanomaterials were used in conjunction with the PCM. From Fig. 18 thermal exergy efficiency is

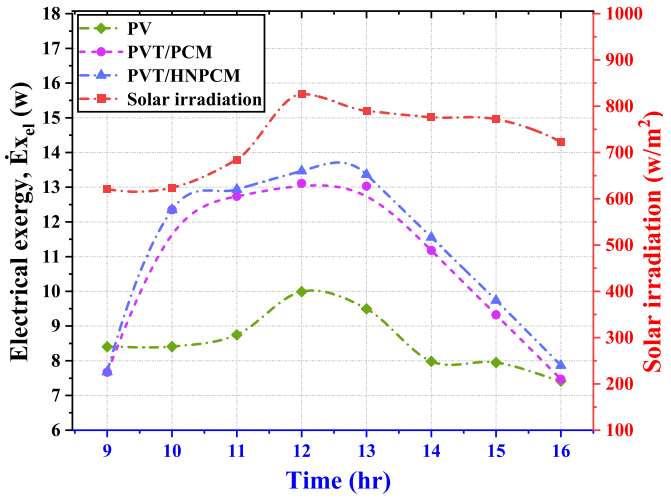

Fig. 15. Variations of output electrical exergy of PV, PVT/PCM, PVT/HNPCM systems.

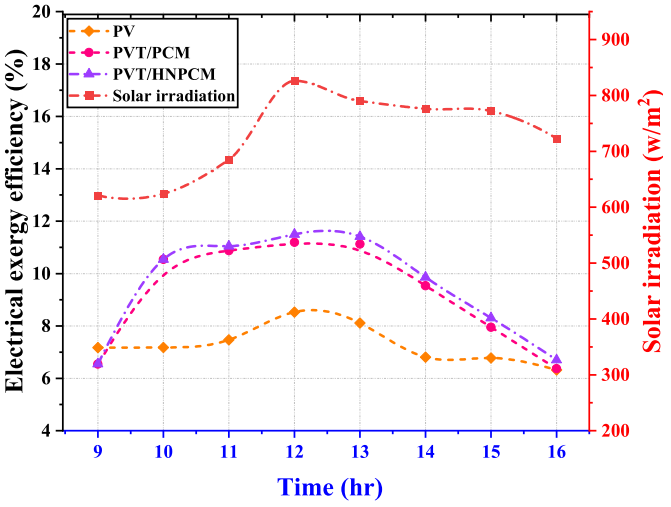

Fig. 16. Variations of output electrical exergy efficiency of PV, PVT/PCM, PVT/HNPCM systems.

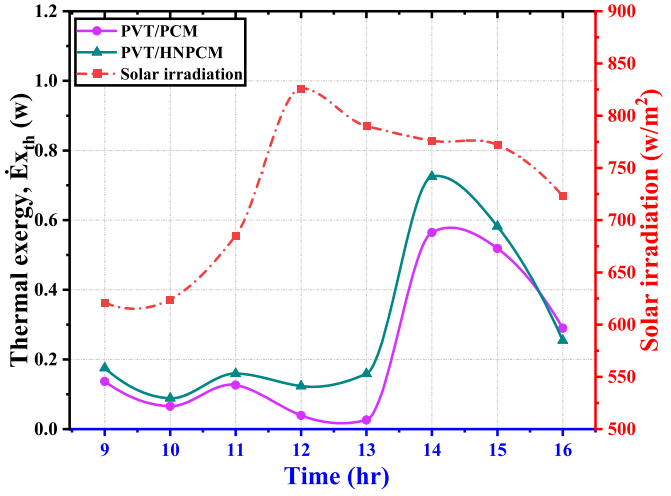

Fig. 17. Variations of output thermal exergy of PV, PVT/PCM, PVT/HNPCM systems.

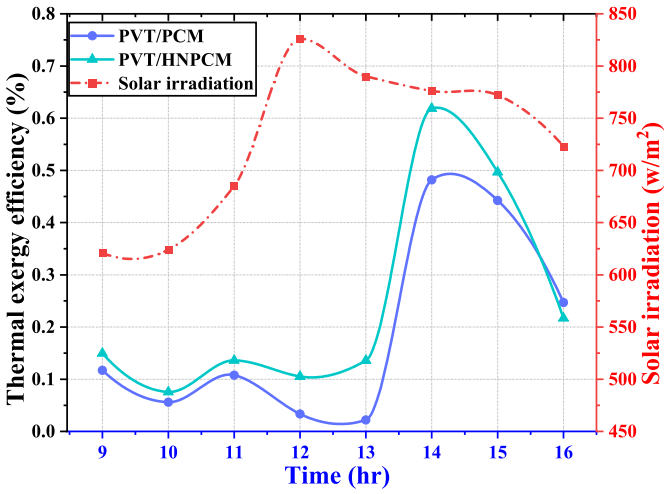

Fig. 18. Variations of output thermal exergy efficiency of PV, PVT/PCM, PVT/HNPCM systems.

0.62 % with PVT/PCM and 0.48 % with PVT/HNPCM system at mass flow rate 0.0021 kg/s. Both the figures elucidate that PVT/HNPCM shows better result for thermal power and efficiency than the PVT/PCM. Additionally, it can be found from Figs. 19 and 20 that the overall exergy and exergy efficiency increased by around 31.61 %, 35.93 %, and 32 %, 36.47 % for PVT/PCM and PVT/HNPCM systems compared to conventional one. PVT/HNPCM shows the emerging result due to the application of nanoparticles are taken place with PCM.

4.8. Cost analysis

The embodied energy calculations are shown in Table 6 and the results of the economic study are shown in Table 7. The findings showed that the modified PV systems (PVT/PCM and PVT/HNPCM) generated DC electricity at a lower cost than traditional PV. This result may be explained by the fact that PVT/PCM and PVT/HNPCM systems generate more net yearly electrical energy than a PV system. Table 7 shows that the cost of producing electricity for PVT/PCM and PVT/HNPCM at an interest rate of 12 % and a lifespan of 10 years was 0.026 and 0.025 $/kWh, respectively, as opposed to 0.03 $/kWh for the PV system; using the proposed PVT/HNPCM system could result in a cost reduction of 16.67 %. These findings show that the PVT/HNPCM system has the greatest economic appeal. However, by incorporating nanoparticles into a hybrid PVT/PCM system for electricity and heat cogeneration, a better economic scenario has attained. Figs. 23 and 24 show the effects of changing the interest rate and PV panel lifetime on the cost of energy and Figs. 21 and 22 show how the annual cost varies over the years at interest rates of 8 %, and 12 %. With interest rates of 8 %, and 12 %, which correspond to lifetimes of 10, 15, and 20 years, the AC is calculated for PV, PVT/PCM, and PVT/HNPCM setups. As predicted, the results showed that, for all PV configurations, the AC falls and grows with an increase in lifetime and interest rate, respectively. In addition, AC for PVT/PCM and PVT/HNPCM configurations were greater than PV configuration in all scenarios taken into consideration due to additional components needed. However, from Table 7, the annual total energy in the case of PVT/HNPCM is significantly greater in comparison with conventional PV, which subsequently causes the reduction of electricity prices. It was found that the cost of producing power for all PV configurations decreases as lifetime increases while rising as interest rates rise. Additionally, the results showed that the PVT/HNPCM system generated DC electricity at a lower cost than standard PV.

4.9. Energy payback time

Table 6 provides more information on the calculations regarding embodied energy for the PV, PVT/PCM, and PVT/HNPCM setups. The results show embodied energy for the PVT/PCM and PVT/HNPCM systems were higher than standard configuration of PV, due to higher material requirements. The modified PVT/HNPCM system, which includes PCM with nanoparticles, a hot water reservoir, and copper pipe layout, has the highest embodied energy. Subsequently for the PV panel having the embodied energy in lower margin. There were 200.40, 244.93 and 249.88 kWh of embodied energy for corresponding PV, PVT/PCM, and PVT/HNPCM systems, respectively. Addition of components increased the embodied energy of the PVT/PCM system by 22.22 % with respect to the reference PV system, while adding hybrid nano-PCM (PVT/HNPCM) increased the embodied energy by 24.69 %. The determination of the amount of time needed to recover the energy and exergy investments made in each configuration is necessary once the embodied energy of each configuration has been calculated. Table 8 shows the calculated energy and exergy-based energy payback time for the PV, PVT/PCM, and PVT/HNPCM configurations. The outcomes showed that the energy based EPBT for the PV, PVT/PCM, and PVT/HNPCM systems were, respectively, 2.29, 0.52, and 0.47 years. While the exergy based EPBT was, respectively, 2.29, 2.13, and 2.10 years. The energy and exergy principles based EPBT of both PVT/PCM, and PVT/HNPCM systems were shorter than that of the PV system. The PVT/HNPCM model shows the convenience having a shorter payback period of 8.29 % compared to conventional PV panel.

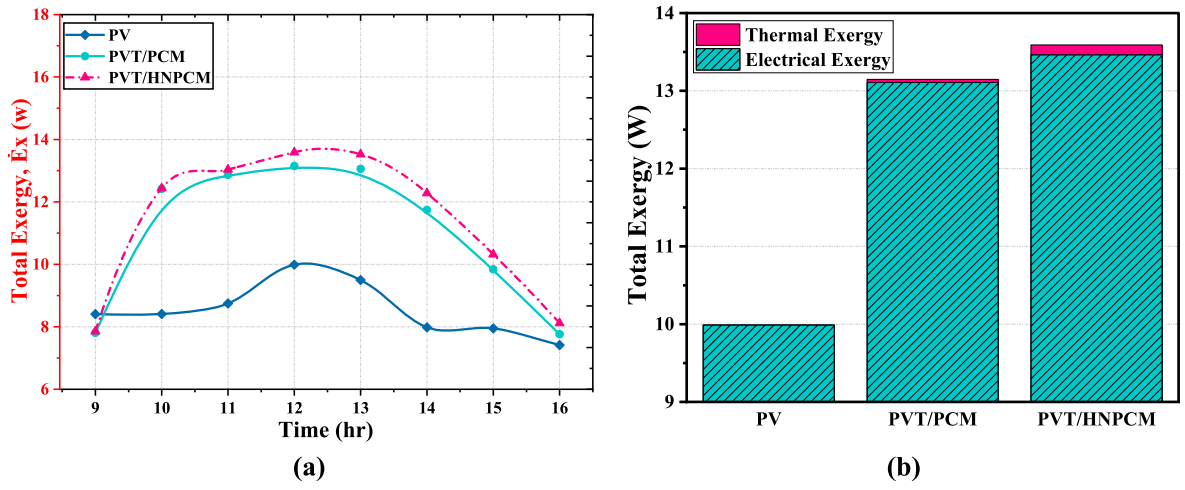

Fig. 19. Variations of (a) total exergy with time, (b) contribution of individual exergies in each of PV, PVT/PCM, PVT/HNPCM systems.

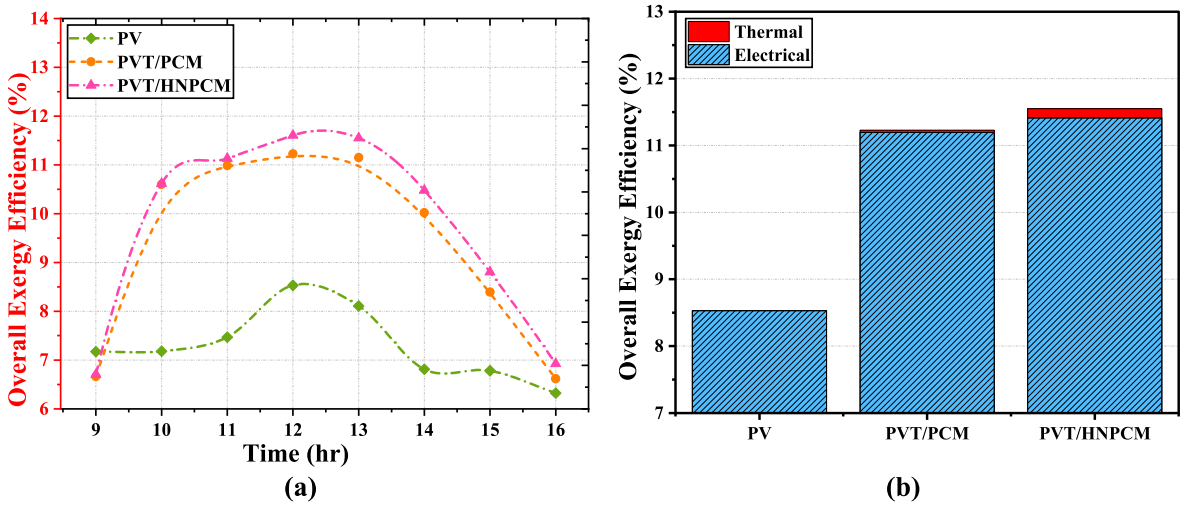

Fig. 20. Variations of (a) oveall exergy with time, (b) contribution of individual overall exergies in each of PV, PVT/PCM, PVT/HNPCM systems.

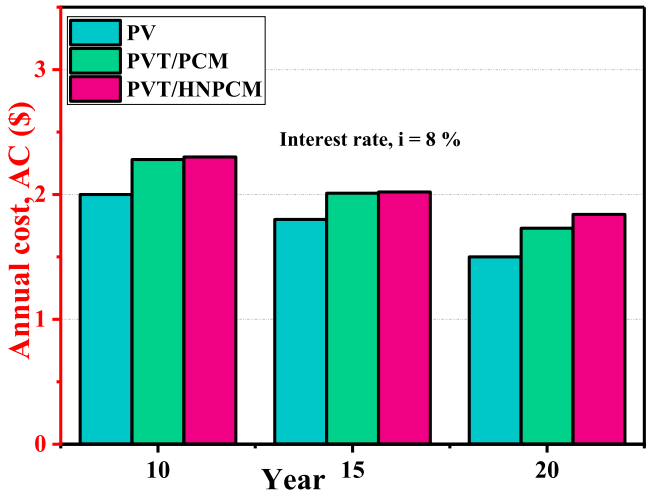

Fig. 21. Variation of AC with respect to the number of years at an interest rate of 8 %.

4.10. Energy production factor analysis

The yearly and lifetime energy production factors are shown in Table 9. If EPF rises, production for any system grows correspondingly. In order to maximize the system's cost-effectiveness, the lifetime value of the EPF need to be as much as possible and should be at least 1. The PVT/PCM and PVT/HNPCM have annual EPF_{ex} values of 0.47 and 0.48, respectively. With a lifespan of 20 years, the PVT/HNPCM system's EPF_{ex} is calculated to be 9.60, which is 9.09 % greater than the EPF_{ex} of a typical PV panel. It makes the suggested system more appealing than conventional systems.

4.11. Life-cycle conversion efficiency

The life cycle conversion efficiency based on exergy estimation for the configurations are shown in Table 10. In this equation, E_{sol} = yearly irradiation × PVT surface area, the annual solar energy is calculated as 695.30 kWh/year. The PVT/HNPCM technology is particularly advantageous as a result of the favorable conversion efficiency for the lifespan. As the difference between the total exergy output (kWh) and embodied energy in the case of PVT/HNPCM in comparison with both PVT/PCM and conventional PV, therefore, the life cycle conversion efficiency is found higher in the case of PVT/HNPCM. The calculated values for LCCE for PVT/PCM panel and PVT/HNPCM systems, respectively, are 0.14 and 0.15. As a result, the PVT/HNPCM system has 36.36 % greater $LCCE_{ex}$ than a typical PV panel. Therefore, it is obvious that the PVT/HNPCM system is more environmentally friendly than the PVT/PCM and PV system only.

4.12. Exergoeconomic evaluation

Table 11 presents the findings of the exergoeconomic evaluation for the PV, PVT/PCM, and PVT/HNPCM setups. It was demonstrated that

Table 6
Calculation of Embodied energy for all three systems (Mishra and Tiwari, 2013; Tiwari and Tiwari, 2016).

Existing components	Energy concentration		Mass of the components (kg)	Embodied energy, Ea (kWh)		
	MJ/kg	kWh/kg		PV	PVT/PCM	PVT/HNPCM
Photovoltaic panel (p-Si)	3276/m^2	910/m^2	0.17 m^2	154.70	154.70	154.70
Al frame	170	47.22	0.20	9.44	9.44	9.44
Glass layer	15	4.16	0.38	1.58	1.58	1.58
Cu pipe	70.60	19.61	0.02	–	0.40	0.40
PCM (Paraffin wax)	42	11.67	2	–	23.30	23.30
Al_2O_3 nanomaterials	200	55.56	0.04	–	–	2.22
ZnO nanomaterials	246	68.33	0.04	–	–	2.73
PVC container	77.90	21.64	0.60	–	12.98	12.98
Hot water storage	50.80	14.11	0.20	–	2.82	2.82
PVC pipes	77.90	21.64	0.20	–	4.33	4.33
Structure	25	6.94	5	34.72	34.72	34.72
Rubber gasket	11.83	3.28	0.20	–	0.66	0.66
Total embodied energy (kWh)				**200.40**	**244.93**	**249.88**

Table 7
Calculation of the Economic parameters of the three configurations.

Existing System	P ($)	CRF ($)	FAC ($)	SSF ($)	S ($)	ASV ($)	AMC ($)	Annual cost, AC ($)	En, annual (kWh/year)	Energy cost, Ce ($/kWh)
PV	13	0.18	2.34	0.06	3.50	0.19	0.35	2.50	87.51	0.03
PVT/PCM	15	0.18	2.70	0.06	4.50	0.26	0.41	2.84	114.14	0.07
PVT/HNPCM	16	0.18	2.88	0.06	5.50	0.31	0.43	2.99	118	0.03

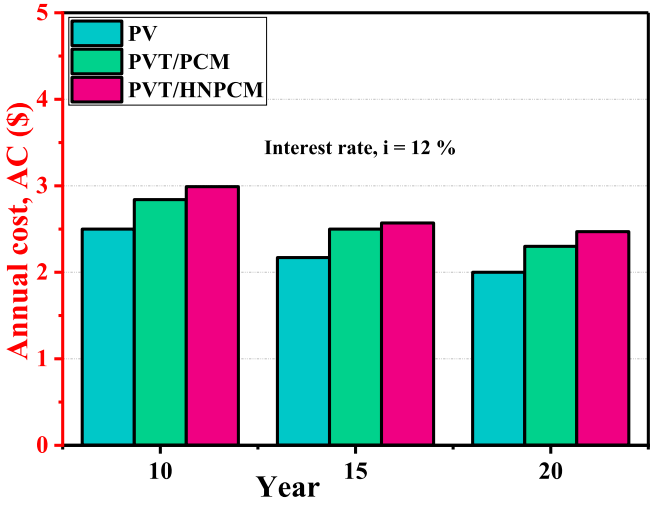

Fig. 22. Variation of AC with respect to the number of years at an interest rate of 12 %.

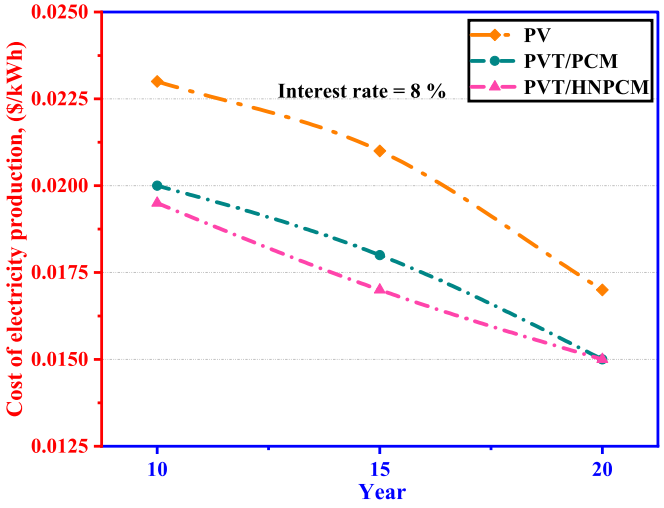

Fig. 23. Variation of the DC electrical energy production cost with number of years at interest rate 8 %.

the exergoeconomic parameter for the PV, PVT/PCM, and PVT/HNPCM configurations was determined to be 35, 40.56, and 39.82 kWh/$, respectively, assuming rate of interest 12 %/year and 10 years lifetime. This result demonstrated that the PVT/HNPCM system has a moderate performance in terms of greater energetic benefit with lower cost, whereas the PV configuration had the worst performance. The PVT/HNPCM system's efficiency from an exergoeconomic perspective, as opposed to PV and PVT/PCM systems, may be understood by the substantial rise in its annual energy savings with an average increment in AC.

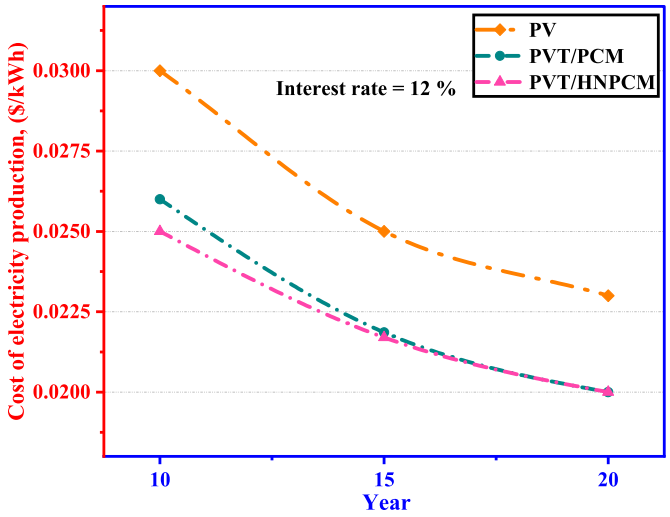

Fig. 24. Variation of the DC electrical energy production cost with number of years at interest rate 12 %.

Table 8
Calculation of EPBT for the three PV setups.

Parameter	PV	PVT/PCM	PVT/HNPCM
Embodied energy, Ea (kWh)	200.40	244.93	249.88
En_{out} (kWh) annual	87.51	470.24	535.15
Ex_{out} (kWh) annual	87.51	115.18	119.05
$EPBT_{en}$	2.29	0.52	0.47
$EPBT_{ex}$	2.29	2.13	2.10

Table 9
Annual and lifetime-based Energy production factor.

System	Ea (kWh)	Ex, out (kWh/year)	EPFex annual	Lifetime	EPF_{ex} life time
PV	200.40	87.51	0.44	20	8.80
PVT/PCM	244.93	115.18	0.47	20	9.40
PVT/HNPCM	249.88	119.05	0.48	20	9.60

Table 10
Calculation of lifecycle conversion efficiency of the three systems.

System	Ea (kWh)	Ex, out (kWh/year)	E_{sol} annual	Life time	$LCCE_{ex}$ life time
PV	200.40	87.51	695.30	20	0.11
PVT/PCM	244.93	115.18	695.30	20	0.14
PVT/HNPCM	249.88	119.05	695.30	20	0.15

4.13. Enviroeconomic evaluation

An environmental assessment based on calculating the CO_2 emissions avoided as a result of using PV, PVT/PCM, and PVT/HNPCM combinations was carried out. Table 12 provides an explanation of the

Table 11
Exergoeconomic investigation for all PV configurations.

System	Time, n (years)	Interest rate, i (%)	AC ($)	Ex_{out} (kWh) annual	Rex (kWh/$)
PV	10	12	2.50	87.51	35
PVT/PCM	10	12	2.84	115.18	40.56
PVT/ HNPCM	10	12	2.99	119.05	39.82

estimated CO_2 avoidance rates considering the proposed three systems using the energy and exergy streams. The findings showed that throughout their full life cycles, the avoided CO_2 for PV, PVT/PCM, and PVT/HNPCM configurations based on the exergy principle, 1.75, 2.30, and 2.38 tons of CO_2 may each be avoided. The PVT/HNPCM configuration was determined to be greener than other configurations based on the aforementioned data. This effect is due to the fact that PVT/HNPCM systems have greater lifetime energy and exergy advantages than PV and PVT/PCM systems. Additionally, Table 12 also provided the results of the environmental economic analysis, which involved setting a carbon price for the configurations that were evaluated. Due to the substantial quantity of mitigated CO_2, as previously shown, the PVT/HNPCM configuration surpassed the others in terms of price values of carbon from an energy and exergy standpoint.

4.14. Sustainability index analysis

Exergy approaches seek to increase effectiveness in order to use resources as effectively as possible while limiting their negative effects. This makes the procedure a useful one for ensuring system sustainability. The sustainability index value can be any positive number between 1 and ∞. In this context, the effectiveness of energy conversion for the following systems conventional PV, PVT/PCM, and PVT/HNPCM was employed to evaluate the sustainability index. The higher the value of the index the more it contains the effectiveness in energy conversion. Sustainability is how the PVT/PCM, PVT/HNPCM systems perform. The sustainability of the system as a result of implantation of nanoparticles with PCM is depicted in Fig. 25. The relationship between the sustainability index and the growth in output exergy is clearly shown. As a result, system performance changed as thermos-chemical properties of PCM changed. The PV, PVT/PCM, and PVT/HNPCM systems have respective total exergy outputs of 87.51, 115.18, and 119.05 kWh/year. As a result, $\psi_{PVT/HNPCM} > \psi_{PVT/PCM} > \psi_{PV}$. Therefore, the sustainability indexes for PV, PVT/PCM, and PVT/HNPCM systems are 1.14, 1.19, and 1.21, respectively. The PVT/HNPCM system was therefore best used under ideal circumstances. The highest sustainability index, 1.21, was attained for PVT/HNPCM system in comparison with the PVT/PCM and PV configurations. As a result, in this experiment, PVT/HNPCM is the most sustainable system. PVT/HNPCM system showed the highest level of sustainability at definite flow rate, followed by PVT/PCM panel, and PV panel. The PVT/HNPCM system was therefore best used under ideal circumstances. The highest sustainability index, 1.21, was attained for PVT/HNPCM system in comparison with the PVT/PCM and PV configurations. As a result, in this experiment, PVT/HNPCM is the most sustainable system. It is evident from the experimental investigation that the higher the exergy efficiency larger the sustainability index. This reflects the maximum utilization of work potential and minimum losses of available energy resources. Therefore, integrating the hybrid nano-PCM into the PVT system offers more sustainable solutions than the PVT/PCM and PV only systems.

Table 12
Environmental and enviro-economic investigation of three PV systems.

Parameter	PV	PVT/ PCM	PVT/ HNPCM
Time (years)	10	10	10
Ex_{out} (kWh) annual	87.51	115.18	119.05
Ex_{out} (kWh) lifetime	875.12	1151.80	1190.50
Exergoenvironmental investigation (Rate ton CO_2)	1.75	2.30	2.38
Exergoenviroeconomic investigation (Rate $)	25.38	33.35	34.51

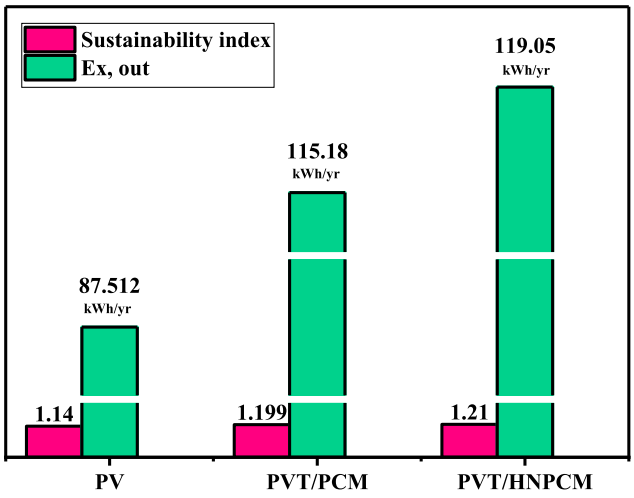

Fig. 25. Variations of sustainability index and exergy output of PV, PVT/PCM, PVT/HNPCM systems.

4.15. Comparison with literature

It is rarely seen for a study to use PVT/HNPCM to examine energy, exergy, exergoeconomic, and enviroeconomic analysis, cost analysis, energy payback time, energy production factor analysis, life-cycle conversion efficiency, and sustainability index analysis all at once. Al_2O_3 nanoparticles combined with paraffin wax are not commonly used in PVT applications. Rather the TES sector prefers to employ this particular type of composite PCM. From the study of (Manigandan and Kumar, 2019) the PVT/PCM/ZnO system showed 7 % higher electrical output compared to convention module and added that PVT/PCM/CuO system has produced 15 % more electrical output than a conventional one. But this study depicts that utilizing hybrid nano Al_2O_3 and ZnO nano particles with PCM makes a higher incremental electrical output about 34.84 %.

With the inclusion of ZnO nano-particles with water to make nanofluid and implemented with PVT system, results showed the electrical and thermal efficiency gained about 14.05 % and 51.66 % (Hosseinzadeh et al., 2018). In contrast, the current study shows, PVT/HNPCM paves the performance in a huge margin with having electrical and thermal efficiencies of 15.56 % and 55 %. However, authors believe that implementing nanofluid to the PVT/HNPCM system can significantly improve performance, and this can be the subject of further investigation. Similar to the previous study, Selimefendigil and Şirin (2022) used CuO nanoparticles with PCM to conduct an investigation of the energy, sustainability, and efficiency indexes. From then, thermal efficiency was close to 46.77 % and electrical efficiency was 10.97 % at lower mass flow rates of water. These show that, in terms of electrical and thermal efficiency, the current study offers approximately 4.59 % and 8.23 % improved efficiencies. Additionally, the sustainability index in the current study is nearly 1.68 % greater than that of the previously mentioned study.

Comparing the three experimental setup reveals that PVT/HNPCM (2.0 wt % Al_2O_3 and ZnO nanoparticles with PCM) performs better than PVT/PCM and conventional PV panel setup. To keep things in perspective, the most compelling findings from the current study been contrasted with those from earlier research that can be found in the

literature. This comparison was based on modification similarities and corresponding percentage improvements, which supports the ability of the system suggested in the current study as shown in Table 13.

5. Conclusions and directions for future study

In this study, PVT systems that combine thermal and photovoltaic collectors for the purpose of producing electricity and heat were designed. The performance of PVT systems is examined in this work in relation to the use of hybrid nano PCM (HNPCM, PCM mixed with Al_2O_3 and ZnO), with varied compositions of 0.5 wt %, 1.0 wt %, and 2.0 wt %. The experiment used a serpentine copper pipe configuration and was conducted outside. Exergy analysis, as a powerful thermodynamic tool which provides an in-depth understanding of the prospective energy availability as well as the positions, actual forms, and magnitudes of the irreversibility and losses of the energy systems. In order to address the pronounced correlation, the PVT systems of this study were compared using exergo-economic parameters in addition to traditional economic ones, taking into account PVT construction, exergo-environmental parameters in addition to standard carbon emission quantification, and sustainability-related parameters like payback period and exergetic sustainability index. The investigation has produced the following conclusions:

- Due to the lack of new chemical bonds, the addition of hybrid nanoparticles into paraffin wax did not alter the original results of pure paraffin wax. For the samples containing mass fractions of hybrid nano-particles of 0.50, 1.0, and 2.0 wt %, respectively, the latent heat capacities were found to be about 234.52 kJ/kg, 232.13 kJ/kg, 230.32 kJ/kg, and 228.93 kJ/kg.
- For the sample with mass fractions of 0.50, 1.0, and 2.0 wt %, the thermal conductivity increased by around 24.68 %, 28.57 %, and 41.56 %, respectively.
- PV, PVT/PCM, and PVT/HNPCM had the highest PV cell temperatures, measuring respectively 61.50 °C, 59.70 °C, and 56.10 °C. This indicates that incorporating hybrid nano-particles with PCM reduces the cell temperature almost 5.40 °C.
- The highest available electrical efficiencies for the PV, PVT/PCM, and PVT/HNPCM systems, were 11.54 %, 15.15 %, and 15.56 %, respectively. Similar trends were about to achieve for electrical exergy efficiency ranging 8.50–11.50 %, which indicates the incremental electrical exergy efficiency is about 35.29 %.
- At a mass flow rate of 0.0021 kg/s, thermal efficiency is 55 % with a PVT/HNPCM system. However, among the three arrangement PVT/HNPCM was the ideal setup for this experiment, resulting in a total exergy efficiency of 13.59 %.
- The cost of producing electricity for PVT/PCM and PVT/HNPCM systems was found to be 0.026 and 0.025 $/kWh, as opposed to 0.03 $/kWh for the PV system.
- The energy based EPBT for the PV, PVT/PCM, and PVT/HNPCM systems were, respectively, 2.29, 0.52, and 0.47 years. While the exergy based EPBT was, respectively, 2.29, 2.13, and 2.10 years. The energy and exergy principles based EPBT of both PVT/PCM, and PVT/HNPCM systems were shorter than that of the PV system.
- The PVT/PCM and PVT/HNPCM have annual EPFex values of 0.47 and 0.48, respectively. With a lifespan of 20 years, the PVT/HNPCM system's EPFex is calculated to be 9.60, which is 9.09 % greater than the EPFex of a typical PV panel. It makes the suggested system more appealing than conventional systems.
- The calculated values for LCCE for PVT/PCM panel and PVT/HNPCM systems, respectively, are 0.14 and 0.15. As a result, the PVT/HNPCM system has 36.36 % greater $LCCE_{ex}$ than a typical PV panel. The PVT/HNPCM technology is particularly advantageous as a result of the favorable conversion efficiency for the lifespan.
- The exergoeconomic parameter for the PV, PVT/PCM, and PVT/HNPCM configurations was determined to be 35.00, 40.56, and 39.82 kWh/$, respectively, assuming rate of interest 12 %/year and 10 years lifetime.
- The findings showed that throughout their full life cycles, PV, PVT/PCM, and PVT/HNPCM configurations based on the exergy principle, 1.75, 2.30, and 2.38 tons of CO_2 may each be avoided. The PVT/HNPCM configuration was determined to be greener than other configurations based on the aforementioned data. The highest sustainability index, 1.21, was attained for PVT/HNPCM system.

It is possible to carry out numerical simulations utilizing computational fluid dynamics techniques to validate experimental results in next investigations. In fact, it is discovered that exergy analysis requires the application of optimization and machine learning algorithms in order to assess the viability from a technical and financial standpoint as well as the potential effects on the environment or the active system. In addition to that the impacts of seasonal variations and degradation of solar PV on the HNPCM system performance require further investigation. To further improve the hybrid PCM-assisted PVT system, the impacts of using alternative fins, geometrical adjustments, and nanoparticles can be examined. However, authors believe that implementing nanofluid to the PVT/HNPCM system can significantly improve performance, and this can be the subject of further investigation. Furthermore, determination and comparing the annual revenue generation amount to

Table 13
Comparison of the present work with the previous studies.

References	Country	Configurations	Improved efficiency		
			Electrical	Thermal	Exergy
Zuhur et al. (2019)	Egypt	Usage of paraffin/aluminum foam (AF) composite underneath the PV panel and comparative analysis with conventional PV and PV/PCM system.	14 %	–	14.97 %
Moein-Jahromi et al. (2022)	Iran	PV panels with the intended heat sinks and an individual panel without a heat sink were set up so that tests were conducted on the single panel's performance in addition to panels with heat sinks of various weight fractions (1, 2, and 3 %). Hybrid NePCM is the result of combining GNP-CuO 3% with Polyethylene Glycol 1500.	13 %	–	–
Çiftçi et al. (2021)	Turkey	Installation of two different collectors with PV panel viz. the serpentine (PV/T1) and the channeled (PV/T2) block.	10.19 %	49.68 %	11.53 %
Bayat et al. (2018)	Iran	Incorporation of ZnO/water nano-fluid along with paraffin wax as PCM underneath the PV panel and comparison with PV and PVT configuration.	14.05 %	51.66 %	13.61 %
Aberoumand et al. (2018)	Algeria	Usage of TiO_2-water nanofluid through the rectangular channel underneath the PV panel.	13.80 %	37.51 %	12.68 %
Ould-Lahoucine et al. (2021)	Iran	Usage of coolant fluids (pure water, 100 % ethylene glycol (EG), mixture with EG (50 %) and water) integrated with PCM with glazed unglazed PVT system.	14.17 %	71.29 %	14.12 %
Present work [a]	Bangladesh	PVT system, passive cooling with paraffin wax (PCM) incorporating hybrid nanoparticles (Al_2O_3 and ZnO) 2.0 wt %.	15.56 %	55 %	11.60 %

[a] Compared to the relevant baseline (conventional) scenario.

previous studies will be a worthwhile research path. To explain further, it is important to emphasize that further research is needed to thoroughly examine the potential risks of NePCM because their environmental effects are not well recognized. In addition to the issues brought above, there can be repercussions for how these materials are disposed of and possible harm to ecosystems and species in the case of spills or leaks. However, advantages beyond energy savings are also available. For instance, NePCM can be constructed with renewable resources and be used to store and use solar energy or waste heat that would otherwise be thrown away. Additionally, research shows that it is unlikely to choose an individual flow rate throughout the experiment. Thus, variation in performance due to diverse flow rate will be investigated in further study.

Author Contributions

Md.Golam Kibria: Writing – review & editing, Writing – original draft, Methodology, Investigation, Conceptualization. Md. Shahriar Mohtasim: Writing – review & editing, Writing – original draft, Investigation, Methodology, Visualization. Barun K. Das: Writing – review & editing, Supervision. Utpol K. Paul: Visualization, Methodology, Formal analysis, Data curation, Writing – original draft. R. Saidur: Writing – review & editing, Investigation

Declaration of competing interest

The authors declare that they have no known competing financial interests or personal relationships that could have appeared to influence the work reported in this paper.

Data availability

Data will be made available on request.

Nomenclature

V_{max}	maximum voltage
A_c	area of solar panel (m^2)
I_{max}	maximum current
C_e	cost of DC electrical energy production
$\ddot{G}$	rate of solar irradiation (W/m^2)
$\dot{E}_{el}$	electrical power (W)
$\dot{m}_f$	mass flow rate of the coolant
V_{oc}	open circuit voltage (V)
$C_{p,f}$	specific heat of the fluid
I_{sc}	short circuit current (A)
$T_{f,out}$	outlet temperature of the fluid
FF	fill factor
$T_{f,in}$	inlet temperature of the fluid
$\dot{E}_{sun}$	sun energy
$\dot{E}_{th}$	thermal power (W)
$\dot{E}x_{el}$	electrical exergy
T_{amb}	ambient temperature
$\dot{E}x_{th}$	thermal exergy
T_{sun}	sun temperature
$\dot{E}x_{sun}$	sun exergy
En_{out}	annual energy output (kwh)
$E_{a,in}$	embodied energy

Symbols

L	life of the system (year)
τ_g	glass transmissivity
E_{sol}	annual solar energy
α_{cell}	cell absorptivity
P	capital cost
η_{ov}	overall electrical efficiency
CRF	capital recovery factor
η_{el}	electrical efficiency
FAC	first annual cost
η_{th}	thermal efficiency
i	interest rate
ε_{th}	thermal exergy efficiency
ASV	annual salvage value
ε_{el}	electrical exergy efficiency
$\dot{G}$	solar irradiation (W)
ε_{ov}	overall exergy efficiency
R_{ex}	exergoeconomic parameter
α_{co_2}	conversion factor (kg/kwh)
Z_{co_2}	enviro-economic parameter

φ_{co_2}	environmental parameter
En_{annual}	annual total energy
SI	sustainability index
z_{co_2}	global carbon value
ψ	thermal exergy rate
Ex_{out}	total exergy out

Subscripts

S	salvage value ex regarding exergy as base
SFF	sinking fund factor en regarding energy as base

References

Abdulmunem, A.R., Mohd Samin, P., Abdul Rahman, H., Hussien, H.A., Izmi Mazali, I., Ghazali, H., 2021. Numerical and experimental analysis of the tilt angle's effects on the characteristics of the melting process of PCM-based as PV cell's backside heat sink. Renew. Energy 173. https://doi.org/10.1016/j.renene.2021.04.014.

Allouhi, A., Rehman, S., Buker, M.S., Said, Z., 2022. Up-to-date literature review on Solar PV systems: technology progress, market status and R&D. J. Clean. Prod. 362 https://doi.org/10.1016/j.jclepro.2022.132339.

Abdalla, A.N., Shahsavar, A., 2023. An experimental comparative assessment of the energy and exergy efficacy of a ternary nanofluid-based photovoltaic/thermal system equipped with a sheet-and-serpentine tube collector. J. Clean. Prod. 395, 136460. https://doi.org/10.1016/j.jclepro.2023.136460.

Abdelrazik, A.S., Al-Sulaiman, F.A., Saidur, R., 2022. Feasibility study for the integration of optical filtration and nano-enhanced phase change materials to the conventional PV-based solar systems. Renew. Energy 187. https://doi.org/10.1016/j.renene.2022.01.095.

Ahmadinejad, M., Soleimani, A., Gerami, A., 2022. The effects of a novel baffle-based collector on the performance of a photovoltaic/thermal system using SWCNT/Water nanofluid. Therm. Sci. Eng. Prog. 34 https://doi.org/10.1016/j.tsep.2022.101443.

Aberoumand, S., Ghamari, S., Shabani, B., 2018. Energy and exergy analysis of a photovoltaic thermal (PV/T) system using nanofluids: an experimental study. Sol. Energy 165. https://doi.org/10.1016/j.solener.2018.03.028.

Abo-Elfadl, S., Yousef, M.S., Hassan, H., 2021. Energy, exergy, economic and environmental assessment of using different passive condenser designs of solar distiller. Process Saf. Environ. Protect. 148 https://doi.org/10.1016/j.psep.2020.10.022.

Abdo, S., Saidani-Scott, H., Abdelrahman, M.A., 2021. Numerical study with eco-exergy analysis and sustainability assessment for a stand-alone nanofluid PV/T. Therm. Sci. Eng. Prog. 24, 100931 https://doi.org/10.1016/J.TSEP.2021.100931.

Borri, E., Zsembinszki, G., Cabeza, L.F., 2021. Recent developments of thermal energy storage applications in the built environment: a bibliometric analysis and systematic review. Appl. Therm. Eng. 189 https://doi.org/10.1016/j.applthermaleng.2021.116666.

Bassam, A.M., Sopian, K., Ibrahim, A., Al-Aasam, A.B., Dayer, M., 2023. Experimental analysis of photovoltaic thermal collector (PVT) with nano PCM and micro-fins tube counterclockwise twisted tape nanofluid. Case Stud. Therm. Eng. 45 https://doi.org/10.1016/j.csite.2023.102883.

Bayat, M., Faridzadeh, M.R., Toghraie, D., 2018. Investigation of finned heat sink performance with nano enhanced phase change material (NePCM). Therm. Sci. Eng. Prog. 5 https://doi.org/10.1016/j.tsep.2017.10.021.

Chaichan, M.T., Kazem, H.A., 2018. Single slope solar distillator productivity improvement using phase change material and Al_2O_3 nanoparticle. Sol. Energy 164, 370–381. https://doi.org/10.1016/J.SOLENER.2018.02.049.

Çiftçi, E., Khanlari, A., Sözen, A., Aytaç, İ., Tuncer, A.D., 2021. Energy and exergy analysis of a photovoltaic thermal (PVT) system used in solar dryer: a numerical and experimental investigation. Renew. Energy 180. https://doi.org/10.1016/j.renene.2021.08.081.

Chow, T.T., Pei, G., Fong, K.F., Lin, Z., Chan, A.L.S., Ji, J., 2009. Energy and exergy analysis of photovoltaic-thermal collector with and without glass cover. Appl. Energy 86 (3). https://doi.org/10.1016/j.apenergy.2008.04.016.

Deniz, E., Çınar, S., 2016. Energy, exergy, economic and environmental (4E) analysis of a solar desalination system with humidification-dehumidification. Energy Convers. Manag. 126 https://doi.org/10.1016/j.enconman.2016.07.064.

Ejaz, A., Jamil, F., Ali, H.M., 2022. A novel thermal regulation of photovoltaic panels through phase change materials with metallic foam-based system and a concise comparison: an experimental study. Sustain. Energy Technol. Assessments 49. https://doi.org/10.1016/j.seta.2021.101726.

Eanest Jebasingh, B., Valan Arasu, A., 2020. A comprehensive review on latent heat and thermal conductivity of nanoparticle dispersed phase change material for low-temperature applications. Energy Storage Mater. 24, 52–74. https://doi.org/10.1016/J.ENSM.2019.07.031.

Esfahani, J.A., Rahbar, N., Lavvaf, M., 2011. Utilization of thermoelectric cooling in a portable active solar still - an experimental study on winter days. Desalination 269 (1–3). https://doi.org/10.1016/j.desal.2010.10.062.

Elbar, A.R.A., Yousef, M.S., Hassan, H., 2019. Energy, exergy, exergoeconomic and enviroeconomic (4E) evaluation of a new integration of solar still with photovoltaic panel. J. Clean. Prod. 233 https://doi.org/10.1016/j.jclepro.2019.06.111.

Fayaz, H., Rahim, N.A., Hasanuzzaman, M., Rivai, A., Nasrin, R., 2019. Numerical and outdoor real time experimental investigation of performance of PCM based PVT system. Sol. Energy 179. https://doi.org/10.1016/j.solener.2018.12.057.

Gad, R., Mahmoud, H., Ookawara, S., Hassan, H., 2023. Evaluation of thermal management of photovoltaic solar cell via hybrid cooling system of phase change material inclusion hybrid nanoparticles coupled with flat heat pipe. J. Energy Storage 57. https://doi.org/10.1016/j.est.2022.106185.

Gelis, K., Celik, A.N., Ozbek, K., Ozyurt, O., 2022. Experimental investigation into efficiency of SiO2/water-based nanofluids in photovoltaic thermal systems using response surface methodology. Sol. Energy 235, 229–241. https://doi.org/10.1016/j.solener.2022.02.021.

Hosseinzadeh, M., Sardarabadi, M., Passandideh-Fard, M., 2018. Energy and exergy analysis of nanofluid based photovoltaic thermal system integrated with phase change material. Energy 147. https://doi.org/10.1016/j.energy.2018.01.073.

Hossain, M.S., Pandey, A.K., Selvaraj, J., Rahim, N.A., Islam, M.M., Tyagi, V.V., 2019. Two side serpentine flow based photovoltaic-thermal-phase change materials (PVT-PCM) system: energy, exergy and economic analysis. Renew. Energy 136. https://doi.org/10.1016/j.renene.2018.10.097.

Hassan, H., S. Yousef, M., Abo-Elfadl, S., 2021. Energy, exergy, economic and environmental assessment of double pass V-corrugated-perforated finned solar air heater at different air mass ratios. Sustain. Energy Technol. Assessments 43. https://doi.org/10.1016/j.seta.2020.100936.

Hassan, H., Yousef, M.S., Fathy, M., Ahmed, M.S., 2020. Impact of condenser heat transfer on energy and exergy performance of active single slope solar still under hot climate conditions. Sol. Energy 204. https://doi.org/10.1016/j.solener.2020.04.026.

Islam, M.M., Hasanuzzaman, M., Rahim, N.A., Pandey, A.K., Rawa, M., Kumar, L., 2021. Real time experimental performance investigation of a NePCM based photovoltaic thermal system: an energetic and exergetic approach. Renew. Energy 172. https://doi.org/10.1016/j.renene.2021.02.169.

Jiakui, C., Abbas, J., Najam, H., Liu, J., Abbas, J., 2023. Green technological innovation, green finance, and financial development and their role in green total factor productivity: empirical insights from China. J. Clean. Prod. 382 https://doi.org/10.1016/j.jclepro.2022.135131.

Jamil, F., Khiadani, M., Ali, H.M., Nasir, M.A., Shoeibi, S., 2023. Thermal regulation of photovoltaics using various nano-enhanced phase change materials: an experimental study. J. Clean. Prod. 414 https://doi.org/10.1016/j.jclepro.2023.137663.

Koohestani, S.S., Nižetić, S., Santamouris, M., 2023. Comparative review and evaluation of state-of-the-art photovoltaic cooling technologies. J. Clean. Prod. 406 https://doi.org/10.1016/j.jclepro.2023.136953.

Kalbande, V.P., Fating, G., Mohan, M., Rambhad, K., Sinha, A.K., 2022. Experimental and theoretical study for suitability of hybrid nano enhanced phase change material for thermal energy storage applications. J. Energy Storage 51, 104431. https://doi.org/10.1016/J.EST.2022.104431.

Kazemian, A., Taheri, A., Sardarabadi, A., Ma, T., Passandideh-Fard, M., Peng, J., 2020. Energy, exergy and environmental analysis of glazed and unglazed PVT system integrated with phase change material: an experimental approach. Sol. Energy 201. https://doi.org/10.1016/j.solener.2020.02.096.

Kazemian, A., Hosseinzadeh, M., Sardarabadi, M., Passandideh-Fard, M., 2018. Experimental study of using both ethylene glycol and phase change material as coolant in photovoltaic thermal systems (PVT) from energy, exergy and entropy generation viewpoints. Energy 162. https://doi.org/10.1016/j.energy.2018.07.069.

Laghari, I.A., Samykano, M., Pandey, A.K., Kadirgama, K., Mishra, Y.N., 2022. Binary composite (TiO2-Gr) based nano-enhanced organic phase change material: effect on thermophysical properties. J. Energy Storage 51, 104526. https://doi.org/10.1016/J.EST.2022.104526.

Liu, L., Niu, J., Wu, J.Y., 2023. Improving energy efficiency of photovoltaic/thermal systems by cooling with PCM nano-emulsions: an indoor experimental study. Renew. Energy 203. https://doi.org/10.1016/j.renene.2022.12.090.

Li, B., Hong, W., Li, H., Lan, J., Zi, J., 2022. Optimized energy distribution management in the nanofluid-assisted photovoltaic/thermal system via exergy efficiency analysis. Energy 242. https://doi.org/10.1016/j.energy.2021.123018.

Mahdi, J.M., Mohammed, H.I., Talebizadehsardari, P., 2021. A new approach for employing multiple PCMs in the passive thermal management of photovoltaic modules. Sol. Energy 222. https://doi.org/10.1016/j.solener.2021.04.044.

M, R., S, L.S., R, H.A., A, D., 2019. Experimental investigation on the abasement of operating temperature in solar photovoltaic panel using PCM and aluminium. Sol. Energy 188. https://doi.org/10.1016/j.solener.2019.05.067.

Manigandan, S., Kumar, V., 2019. Comparative study to use nanofluid ZnO and CuO with phase change material in photovoltaic thermal system. Int. J. Energy Res. 43 (5), 1882–1891. https://doi.org/10.1002/ER.4442.

Mishra, R.K., Tiwari, G.N., 2013. Energy matrices analyses of hybrid photovoltaic thermal (HPVT) water collector with different PV technology. Sol. Energy 91. https://doi.org/10.1016/j.solener.2013.02.002.

Moein-Jahromi, M., Rahmanian-Koushkaki, H., Rahmanian, S., Pilban Jahromi, S., 2022. Evaluation of nanostructured GNP and CuO compositions in PCM-based heat sinks for photovoltaic systems. J. Energy Storage 53, 105240. https://doi.org/10.1016/J.EST.2022.105240.

Nasr Esfahani, M., Aghdam, A.H., Refahi, A., 2023. Energy, exergy, exergoeconomic, exergoenvironmental (4E) assesment, sensitivity analysis and multi-objective optimization of a PTC –tehran climate data case study. J. Clean. Prod. 415 https://doi.org/10.1016/j.jclepro.2023.137821.

Nematpour Keshteli, A., Sheikholeslami, M., 2019. Nanoparticle enhanced PCM applications for intensification of thermal performance in building: a review. J. Mol. Liq. 274 https://doi.org/10.1016/j.molliq.2018.10.151.

Ould-Lahoucine, C., Ramdani, H., Zied, D., 2021. Energy and exergy performances of a TiO2-water nanofluid-based hybrid photovoltaic/thermal collector and a proposed new method to determine the optimal height of the rectangular cooling channel. Sol. Energy 221. https://doi.org/10.1016/j.solener.2021.04.027.

Praveenkumar, S., Agyekum, E.B., Kumar, A., Velkin, V.I., 2023. Thermo-enviro-economic analysis of solar photovoltaic/thermal system incorporated with u-shaped grid copper pipe, thermal electric generators and nanofluids: an experimental investigation. J. Energy Storage 60. https://doi.org/10.1016/j.est.2023.106611.

Park, S.R., Pandey, A.K., Tyagi, V.V., Tyagi, S.K., 2014. Energy and exergy analysis of typical renewable energy systems. Renew. Sustain. Energy Rev. 30 https://doi.org/10.1016/j.rser.2013.09.011.

Shahverdian, M.H., Sohani, A., Zamani Pedram, M., Sayyaadi, H., 2023. An optimal strategy for application of photovoltaic-wind turbine with PEMEC-PEMFC hydrogen storage system based on techno-economic, environmental, and availability indicators. J. Clean. Prod. 384 https://doi.org/10.1016/j.jclepro.2022.135499.

Said, Z., Ahmad, F.F., Radwan, A.M., Hachicha, A.A., 2023a. New thermal management technique for PV module using Mist/PCM/Husk: an experimental study. J. Clean. Prod. 401 https://doi.org/10.1016/j.jclepro.2023.136798.

Soliman, A.S., Zhu, S., Xu, L., Dong, J., Cheng, P., 2021. Design of an H2O-LiBr absorption system using PCMs and powered by automotive exhaust gas. Appl. Therm. Eng. 191 https://doi.org/10.1016/j.applthermaleng.2021.116881.

Said, Z., Sohail, M.A., Pandey, A.K., Sharma, P., Waqas, A., Chen, W.H., Nguyen, P.Q.P., Nguyen, V.N., Pham, N.D.K., Nguyen, X.P., 2023b. Nanotechnology-integrated phase change material and nanofluids for solar applications as a potential approach for clean energy strategies: progress, challenges, and opportunities. J. Clean. Prod. 416 https://doi.org/10.1016/j.jclepro.2023.137736.

Sheikholeslami, M., Mahian, O., 2019. Enhancement of PCM solidification using inorganic nanoparticles and an external magnetic field with application in energy storage systems. J. Clean. Prod. 215 https://doi.org/10.1016/j.jclepro.2019.01.122.

Sardari, P.T., Babaei-Mahani, R., Giddings, D., Yasseri, S., Moghimi, M.A., Bahai, H., 2020. Energy recovery from domestic radiators using a compact composite metal Foam/PCM latent heat storage. J. Clean. Prod. 257 https://doi.org/10.1016/j.jclepro.2020.120504.

Salem, M.R., Elsayed, M.M., Abd-Elaziz, A.A., Elshazly, K.M., 2019. Performance enhancement of the photovoltaic cells using Al2O3/PCM mixture and/or water cooling-techniques. Renew. Energy 138. https://doi.org/10.1016/j.renene.2019.02.032.

Selimli, S., Dumrul, H., Yilmaz, S., Akman, O., 2021. Experimental and numerical analysis of energy and exergy performance of photovoltaic thermal water collectors. Sol. Energy 228. https://doi.org/10.1016/j.solener.2021.09.049.

Sardarabadi, M., Hosseinzadeh, M., Kazemian, A., Passandideh-Fard, M., 2017a. Experimental investigation of the effects of using metal-oxides/water nanofluids on a photovoltaic thermal system (PVT) from energy and exergy viewpoints. Energy 138. https://doi.org/10.1016/j.energy.2017.07.046.

Selimefendigil, F., Şirin, C., 2022. Energy and exergy analysis of a hybrid photovoltaic/thermal-air collector modified with nano-enhanced latent heat thermal energy storage unit. J. Energy Storage 45, 103467. https://doi.org/10.1016/J.EST.2021.103467.

Sardarabadi, M., Passandideh-Fard, M., Maghrebi, M.J., Ghazikhani, M., 2017b. Experimental study of using both ZnO/water nanofluid and phase change material (PCM) in photovoltaic thermal systems. Sol. Energy Mater. Sol. Cells 161. https://doi.org/10.1016/j.solmat.2016.11.032.

Tiwari, S., Tiwari, G.N., 2016. Exergoeconomic analysis of photovoltaic-thermal (PVT) mixed mode greenhouse solar dryer. Energy 114. https://doi.org/10.1016/j.energy.2016.07.132.

Tariq, S.L., Ali, H.M., Akram, M.A., Janjua, M.M., Ahmadlouydarab, M., 2020. Nanoparticles enhanced phase change materials (NePCMs)-A recent review. Appl. Therm. Eng. 176, 115305 https://doi.org/10.1016/J.APPLTHERMALENG.2020.115305.

Wahab, A., Khan, M.A.Z., Hassan, A., 2020. Impact of graphene nanofluid and phase change material on hybrid photovoltaic thermal system: exergy analysis. J. Clean. Prod. 277 https://doi.org/10.1016/j.jclepro.2020.123370.

Yazdanifard, F., Ameri, M., Taylor, R.A., 2020. Numerical modeling of a concentrated photovoltaic/thermal system which utilizes a PCM and nanofluid spectral splitting. Energy Convers. Manag. 215 https://doi.org/10.1016/j.enconman.2020.112927.

Yousef, M.S., Sharaf, M., Huzayyin, A.S., 2022. Energy, exergy, economic, and enviroeconomic assessment of a photovoltaic module incorporated with a paraffin-metal foam composite: an experimental study. Energy 238. https://doi.org/10.1016/j.energy.2021.121807.

Yousef, M.S., Hassan, H., 2019. An experimental work on the performance of single slope solar still incorporated with latent heat storage system in hot climate conditions. J. Clean. Prod. 209 https://doi.org/10.1016/j.jclepro.2018.11.120.

Yousef, M.S., Hassan, H., 2020. Energy payback time, exergoeconomic and enviroeconomic analyses of using thermal energy storage system with a solar desalination system: an experimental study. J. Clean. Prod. 270 https://doi.org/10.1016/j.jclepro.2020.122082.

Yousef, M.S., Hassan, H., Sekiguchi, H., 2019. Energy, exergy, economic and enviroeconomic (4E) analyses of solar distillation system using different absorbing materials. Appl. Therm. Eng. 150 https://doi.org/10.1016/j.applthermaleng.2019.01.005.

Zuhur, S., Ceylan, İ., Ergün, A., 2019. Energy, exergy and environmental impact analysis of concentrated PV/cooling system in Turkey. Sol. Energy 180. https://doi.org/10.1016/j.solener.2019.01.060.